Double Higgs searches at CMS

王锦
中国科学院高能物理研究所

15 July 2026

高能物理第十二届全国会员代表大会

Compact Muon Solenoid

- CMS is a general-purpose detector at the LHC
  - Test Standard Model (SM) predictions
  - Search for new physics beyond the SM

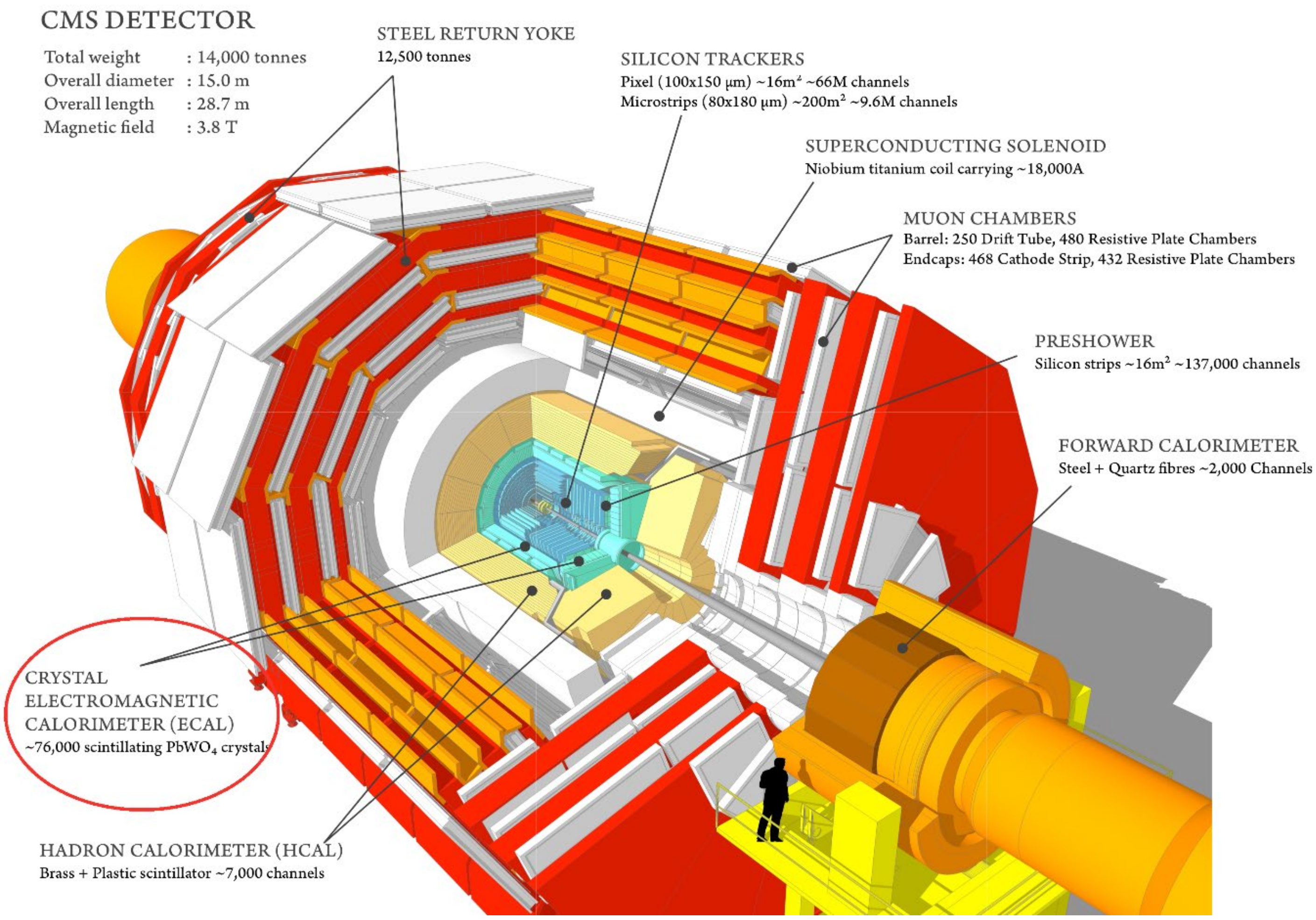

Introduction

- HH measurement directly probes Higgs self-coupling λ
  - Crucial for understanding the Higgs field potential
    - $V(H) = \frac{1}{2} m_H{}^2 H^2 + \lambda_3 H^3 + \lambda_4 H^4$

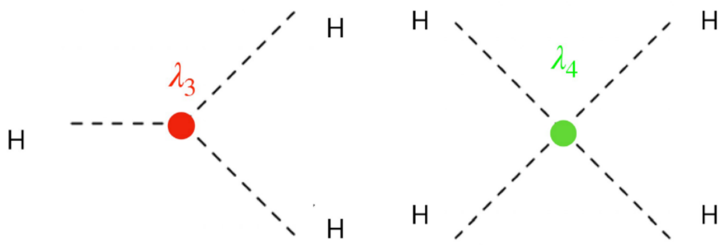

  - Tight correlation with the dynamics of the electroweak phase transition

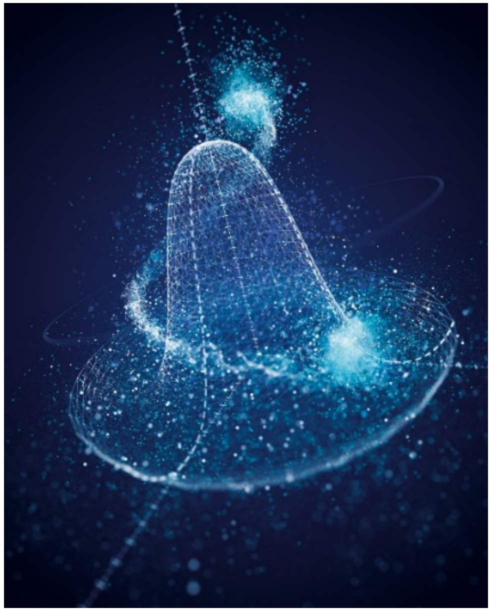

CERN Courier

- HH production also sensitive to Beyond Standard Model (BSM) effects
  - Modified SM couplings
  - Additional couplings in Effective Field Theory
  - Resonant production

HH production

- HH production challenging to measure due to it small cross section
  - $\sigma_{HH} \sim \frac{\sigma_H}{1000}$ in SM at 13TeV
  - Two main production modes
    - $\sigma_{ggF} = 31.1\ fb$ SM @13TeV
      - Dominant channel for studying self-coupling
      - Destructive interference
    - $\sigma_{VBF} = 1.73\ fb$ SM @13TeV
      - Only channel to access quartic VVHH coupling
    - ~11% increase in the cross section at 13.6 TeV
  - Test deviation from the SM couplings with κ-framework: : $k_X = X/X_{SM}$

$\kappa_\lambda = \lambda/\lambda^{SM}$ also dictates signal kinematics:

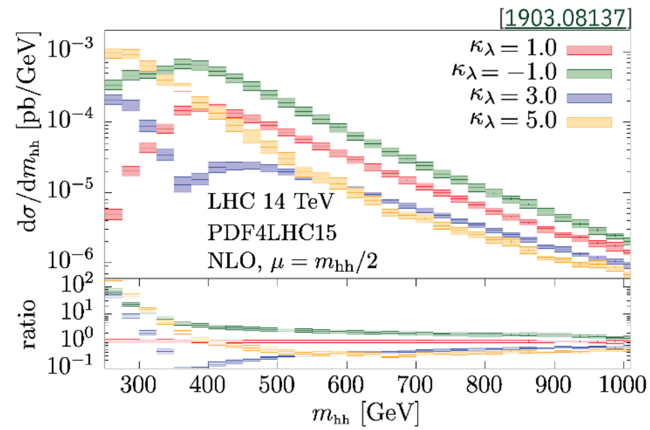

Gluon-gluon fusion (**ggF**)

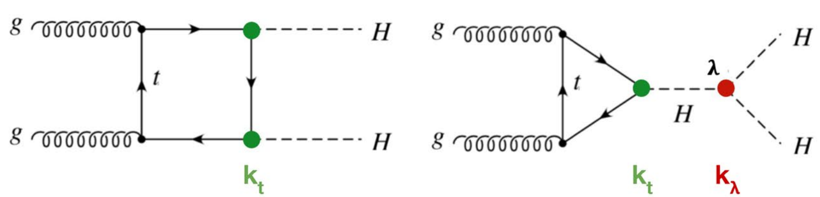

Vector-boson fusion (**VBF**)

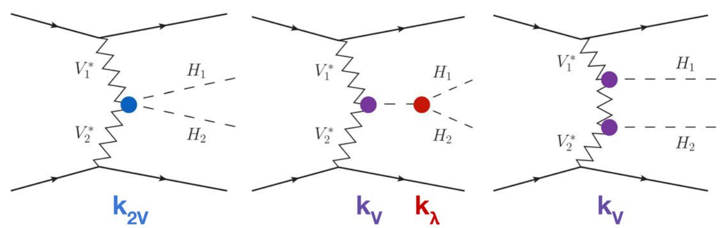

- Additional production modes including VHH, ttHH

Overview of HH measurement at CMS

- HH searches have been evolving since early Run 2
  - More HH production modes and decay channels, boosted topologies
  - Extensive usage of machine learning, trigger, selection and tagging optimization
- Best HH sensitivity via combination of all channels
  - Run2 Legacy Combination : arXiv:2510.07527
  - Using full Run 2 data with 138 fb^{-1}
  - All final states defined to be mutually exclusive

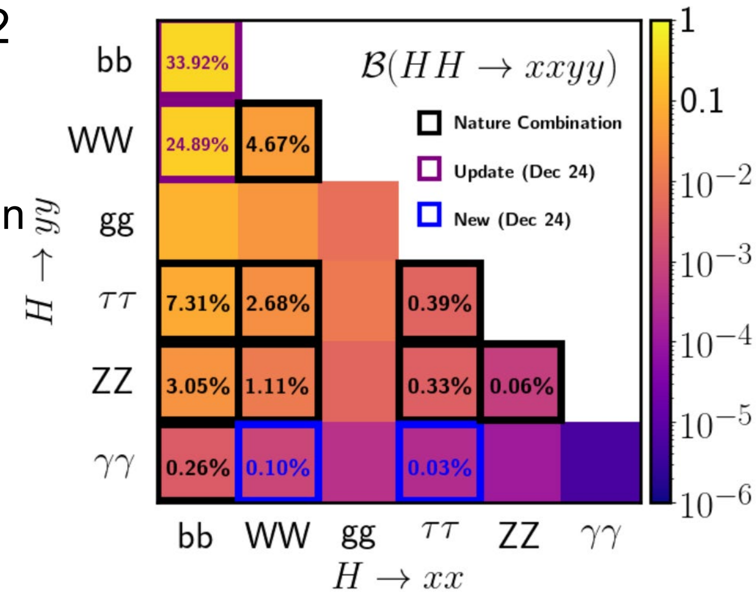

HH Combination Nature 607 (2022) 60		New additions in Run2 Legacy Combination	
$bbbb$ resolved	Phys. Rev. Lett. 129 (2022) 081802	$VHH\ bbbb$	JHEP 10 (2024) 061
$bbbb$ boosted	Phys. Rev. Lett. 131 (2023) 041803	$bbWW(leptonic)$	JHEP 07 (2024) 293
$bb\tau\tau$	Phys. Lett. B 842 (2023) 137531	$bbVV(hadronic)$	CMS-PAS-HIG-23-012
$bb\gamma\gamma$	JHEP03(2021)257	$WW\gamma\gamma$	CMS-PAS-HIG-21-014
$bbZZ(4l)$	JHEP 06 (2023) 130	$\tau\tau\gamma\gamma$	CMS-PAS-HIG-22-012
$Multilepton$	JHEP 07 (2023) 095		

Legacy Run2 combination

- The most complete CMS combination to date
  - Using full Run 2 data with 138 fb^{-1}
  - All available channels in Run2
    - Overlap removal between channels leading to slight shifts in the upper limit compared to individual results
  - Updated uncertainties and signal cross section
  - New EFT interpretations
  - Updated Projections

- Obs.(exp.) upper limit on HH signal strength : $3.5\ (2.5)\ \times \sigma^{HH\ SM}_{ggF+VBF}$
  - Significant improvement comparing to early Run 2 results
    - ~5× improvement, far beyond the ~2× gain expected from luminosity scaling alone.

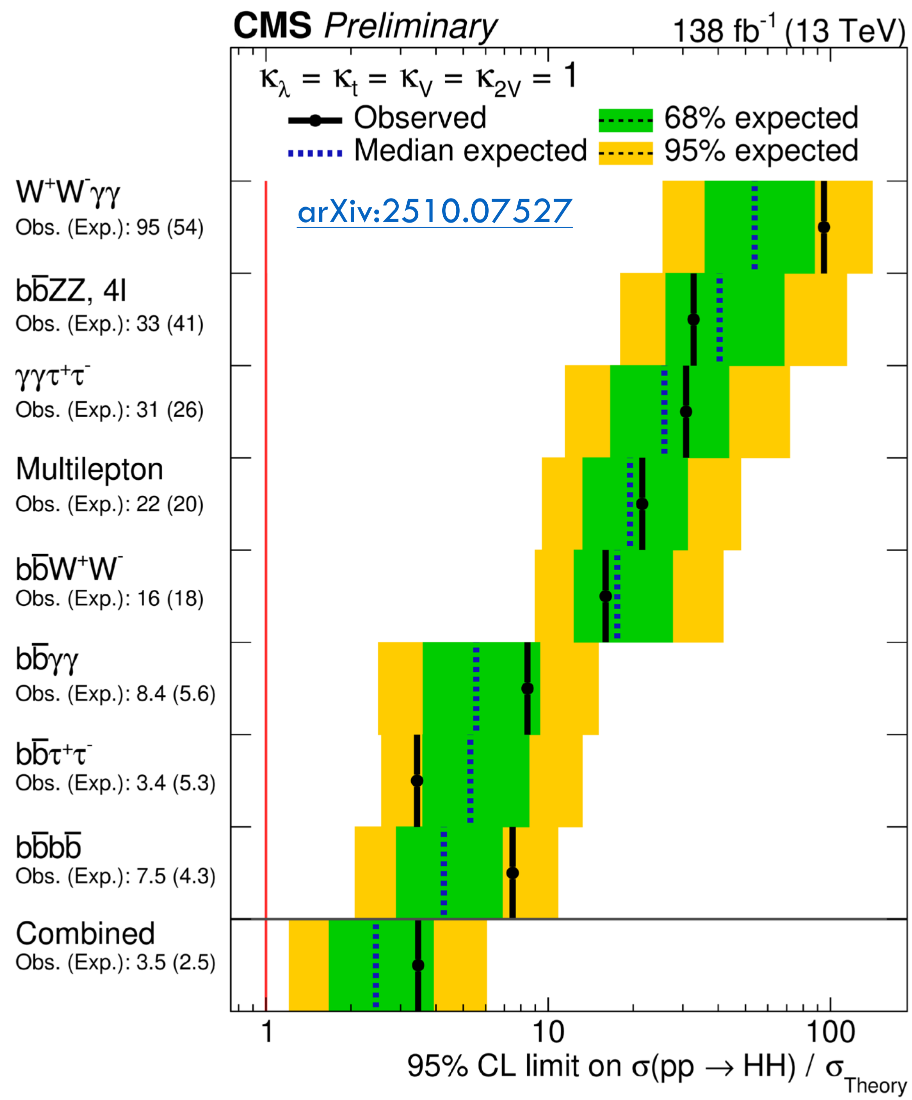

Limits extracted under the background-only hypothesis

Constraints on coupling modifiers

- Constrain Higgs boson self-interaction coupling modifier κ_λ @ 95.4% C.L.
  - Observed (expected) k_λ range: $-1.40\ (-2.29) < k_\lambda < 6.43\ (7.95)$
- Constrain quartic VVHH coupling modifier κ_{2V} @ 95.4% C.L.
  - Observed (expected) k_{2V} range: $0.63\ (0.62) < k_{2V} < 1.40\ (1.41)$
- $k_{2V} = 0$ is excluded with a significance of 6σ, assuming $k_\lambda = k_V = k_t = 1$

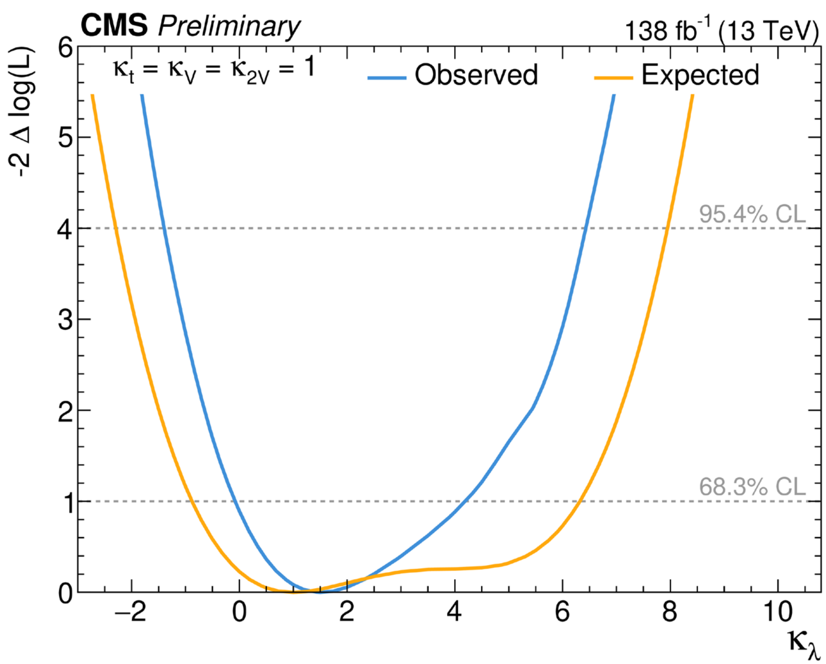

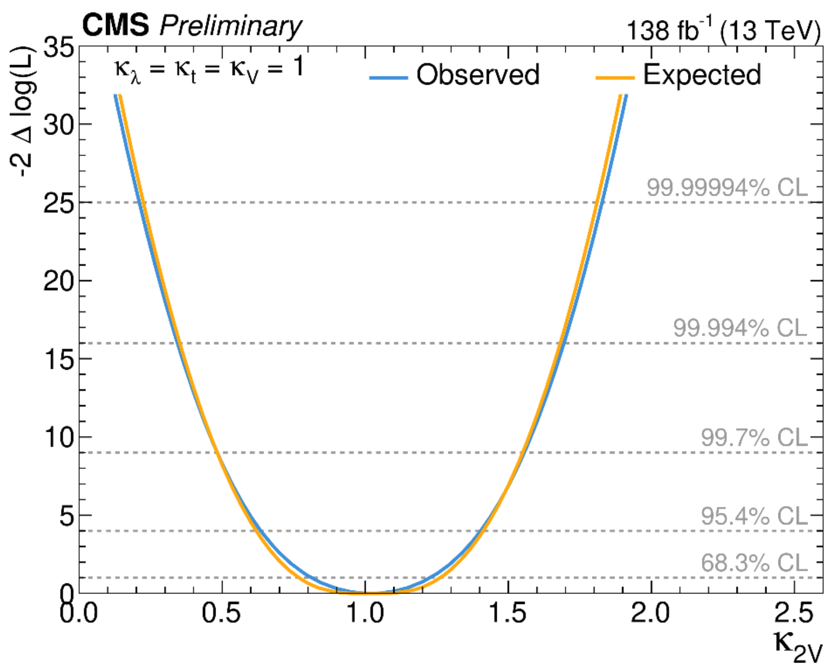

arXiv:2510.07527

2D coupling constraints

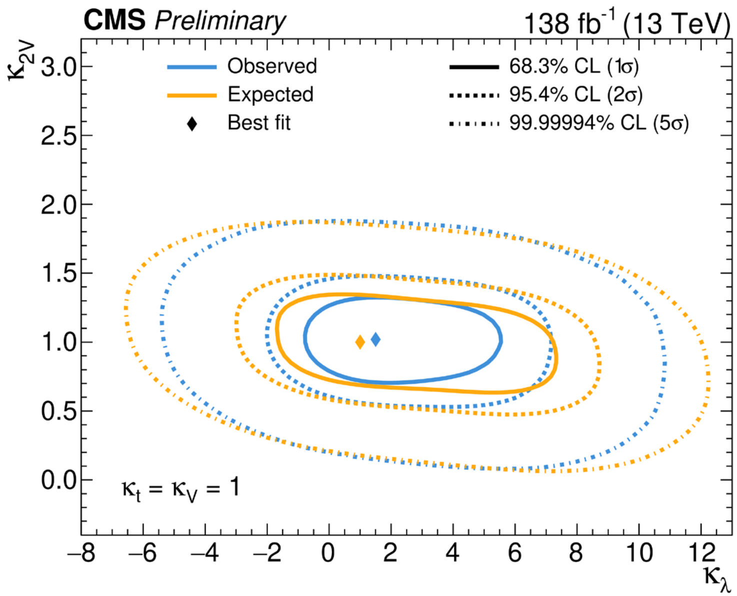

- Two-dimensional constraints in the $(k_\lambda, k_{2V}), (k_\lambda, k_t), (k_V, k_{2V})$ planes
- No significant deviation from the SM is observed

arXiv:2510.07527

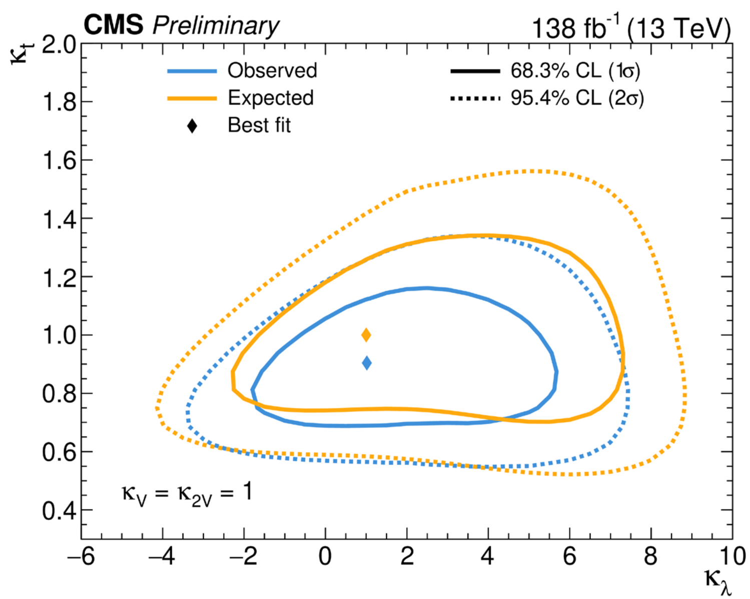

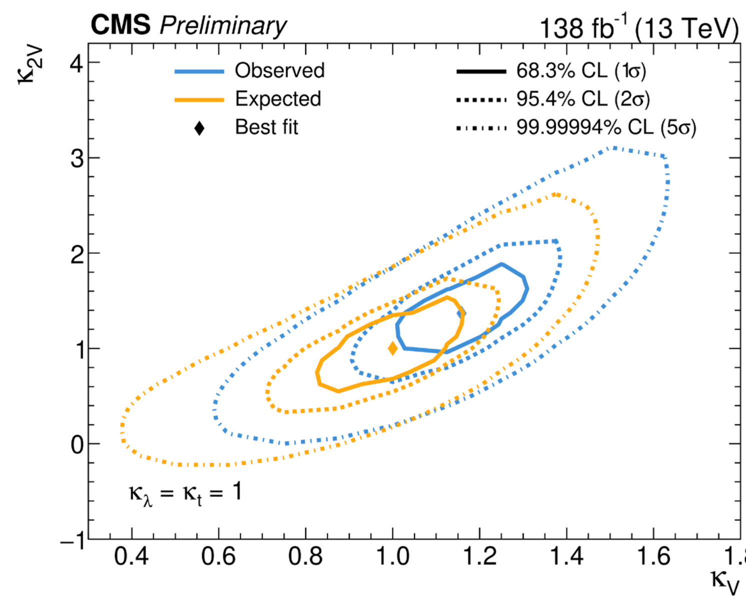

The HEFT modeling in CMS

- New symmetries and/or new heavy particles induces additional effective terms into the H potential

- Studied in the Higgs EFT (HEFT) scenario
  - linear variation of couplings $(k_\lambda, k_t, c_2, c_g, c_{2g})$

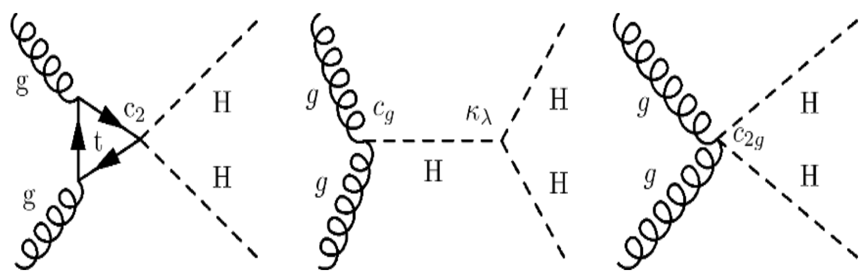

$$|A|^2 = \kappa_\lambda^2 \cdot \kappa_t^2 \cdot |\triangle|^2 + \kappa_t^4 \cdot |\square|^2 + c_2^2 \cdot |X|^2 + \kappa_\lambda \cdot \kappa_t \cdot c_2 \cdot |\triangle^* X + X^* \triangle|$$
$$+ \kappa_t^2 \cdot c_2 \cdot |\square^* X + X^* \square| + \kappa_t^3 \cdot \kappa_\lambda \cdot |\triangle^* \square + \square^* \triangle|$$

HH production amplitude expression including EFT contact term c_2

$\triangle$: triangle diagram contribution

$\square$: box diagram contribution

X: contact interaction from EFT

Upper limits on HEFT benchmarks

- Upper limits in two representative HEFT benchmarks with different combinations of the coupling modifiers ($k_\lambda, k_t, c_2, c_g, c_{2g}$)
  - 1: Thirteen benchmark scenarios spanning a broad range of the coupling variations
  - 2: With NLO precision and considers direct and indirect constraints on couplings
- No significant deviations from expectations are observed
  - An overall small excess in all benchmarks, between 1σ and 2σ

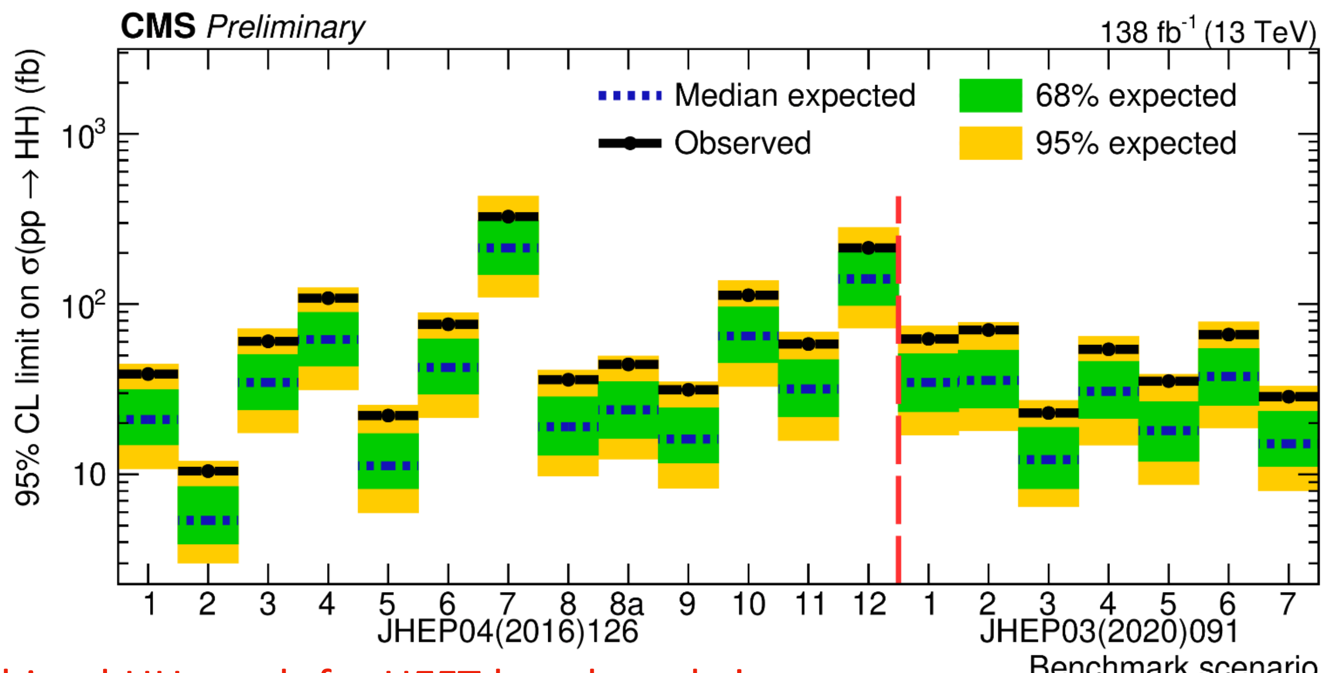

First combined HH result for HEFT benchmarks!

arXiv:2510.07527

HEFT coupling scans

- Scan of C2 coupling modifier
  - In general compatible with the SM
  - The best fit slightly prefers $c_2 = 0.4$

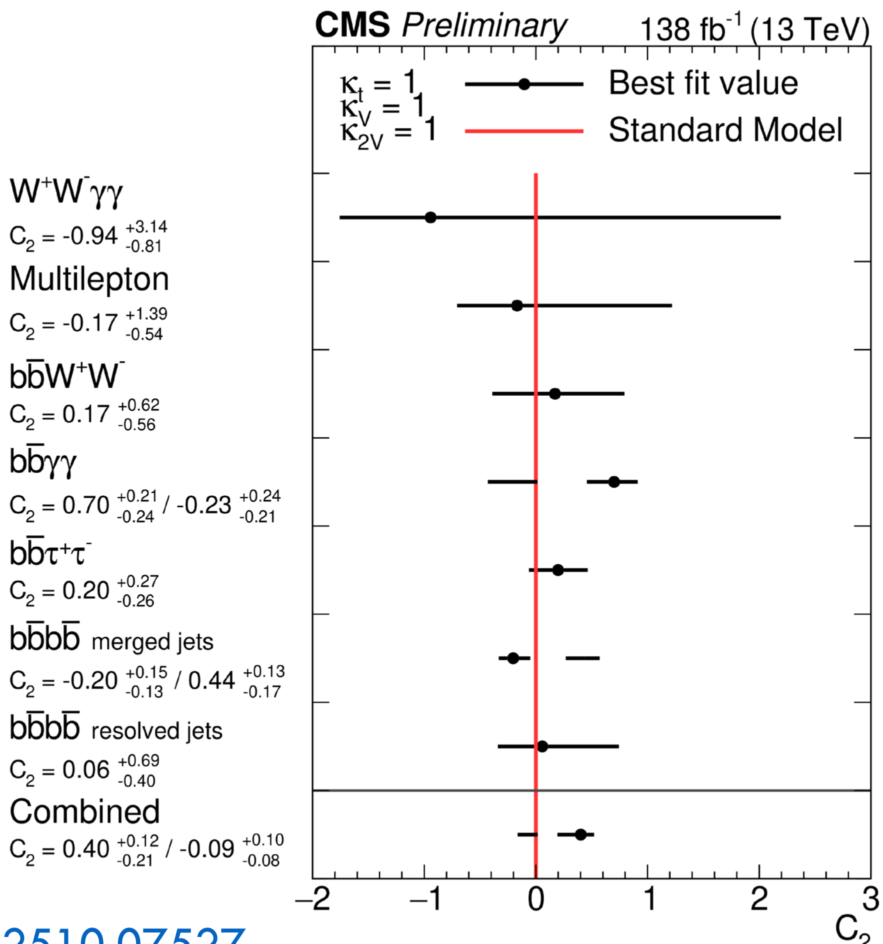

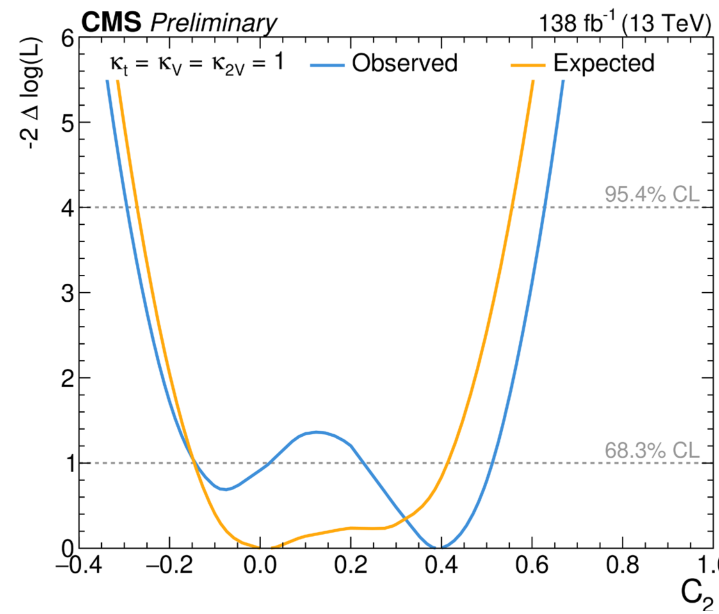

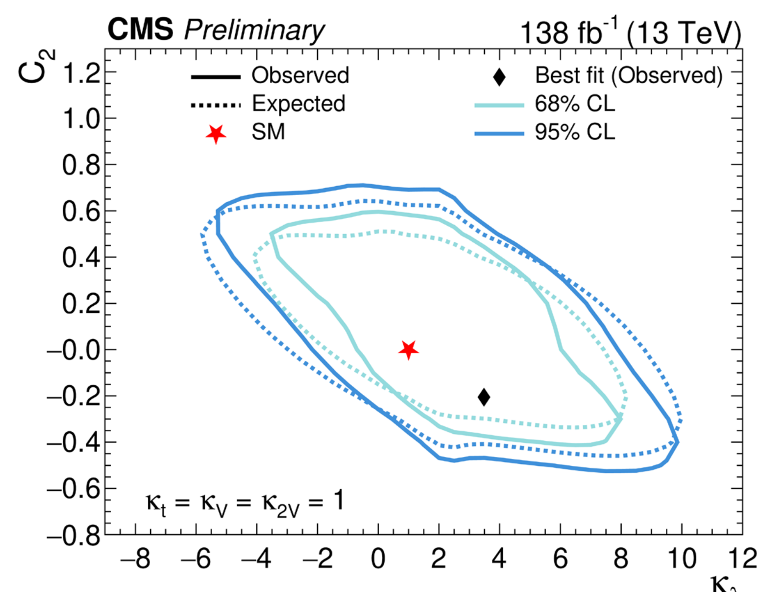

arXiv:2510.07527

UV complete reinterpretations

- Probing UV complete models directly with available HH searches at CMS
  - Model dependent with more physical assumptions about interference, parameter values and correlations
  - A realistic testbed for assessing the reach and limitations of HH searches under explicit UV assumptions
  - Complementary to EFT interpretation and resonant searches
- Explored an example UV mappings for HH from [JHEP 02 (2021) 049]

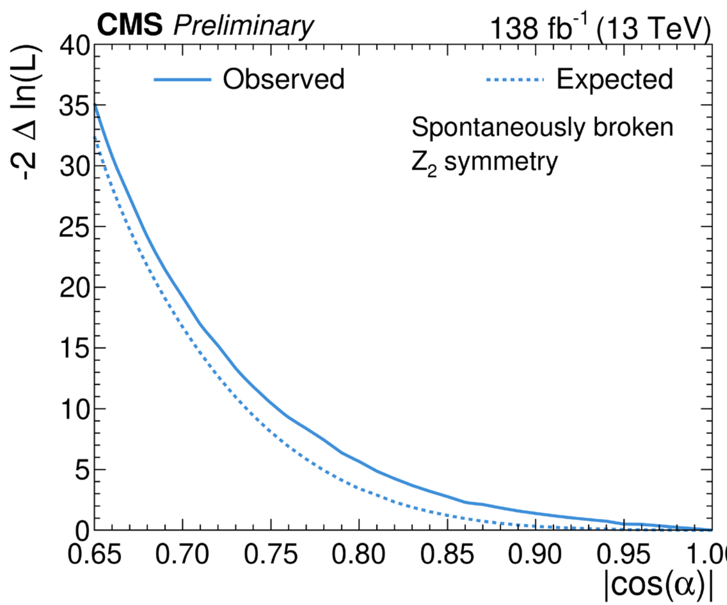

Competitive singlet results

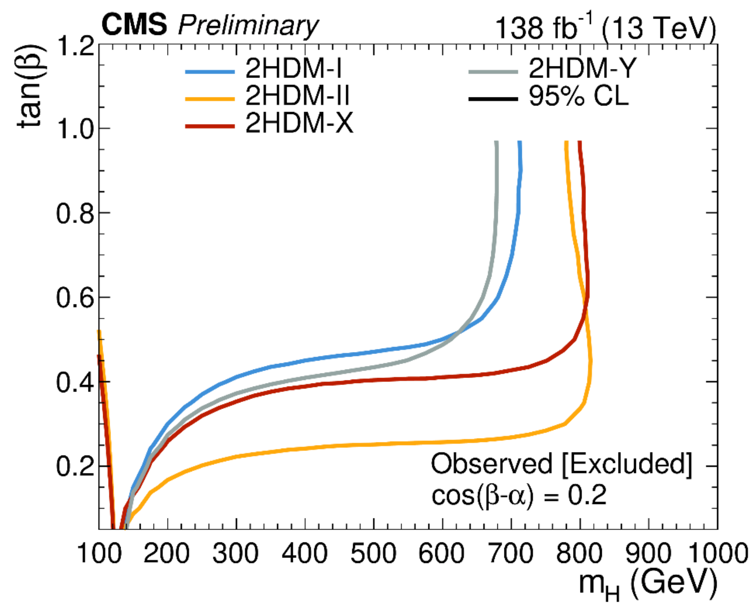

2HDM results: complementary coverage in the high-mass region

arXiv:2510.07527

H+HH combination

- Single Higgs boson processes sensitive to Higgs self-coupling through EW corrections

Single Higgs production vs. k_λ

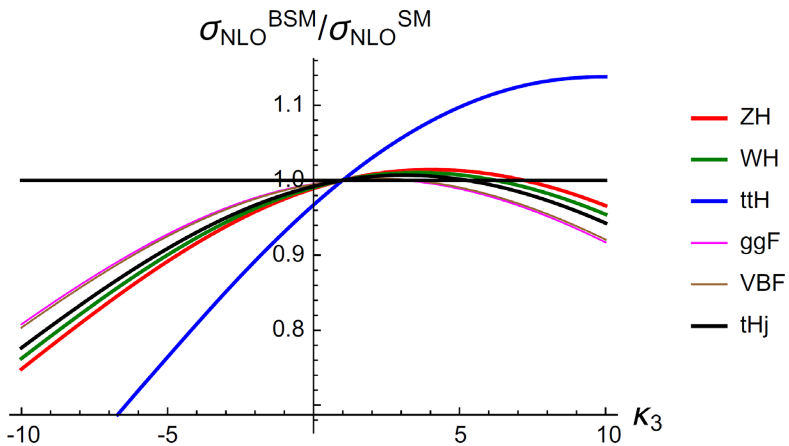

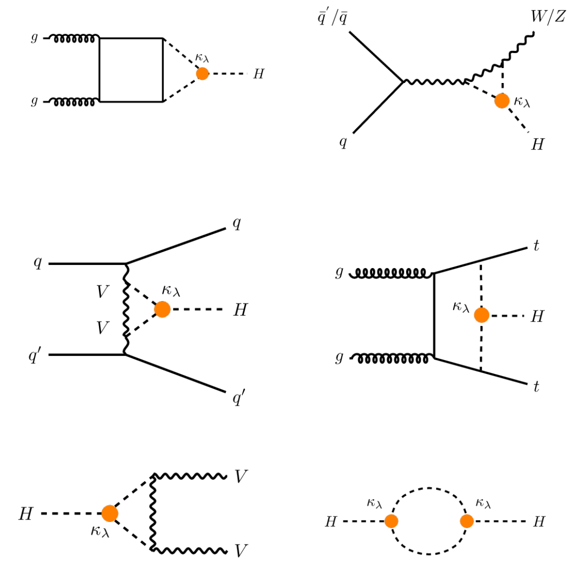

Higgs decay vs. k_λ

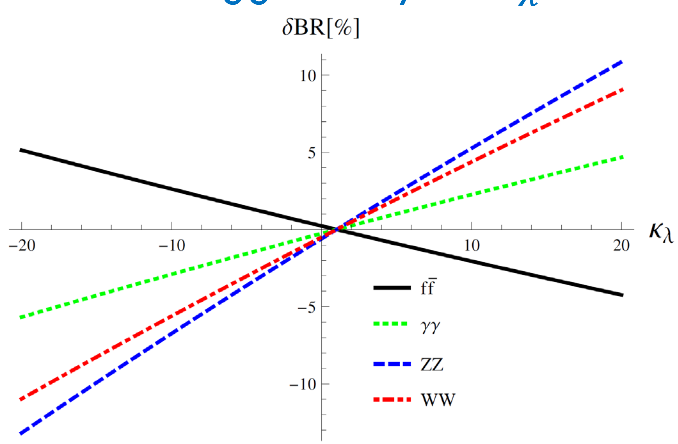

Kinematics vs. k_λ

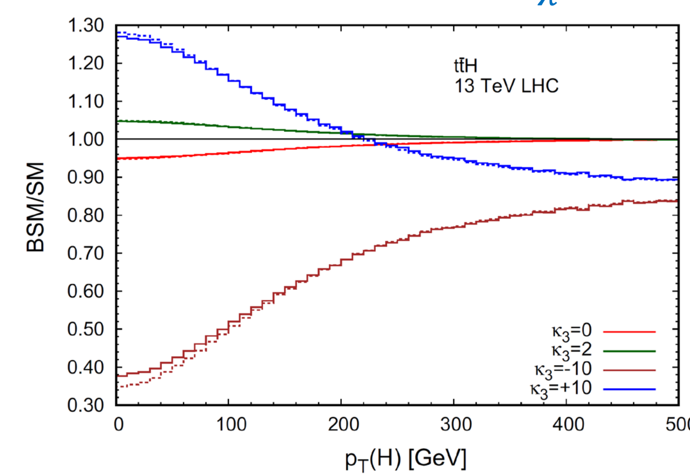

H+HH combination

- Constrain k_λ with H+HH combination at 2 σ confidence level
  - Observed (expected) range fixing other H coupling: $-1.2\ (-2.0) < k_\lambda < 7.5\ (7.7)$
  - Observed (expected) range floating other H coupling: $-1.4\ (-2.3) < k_\lambda < 7.8\ (7.8)$

Phys. Lett. B 861 (2025) 139210

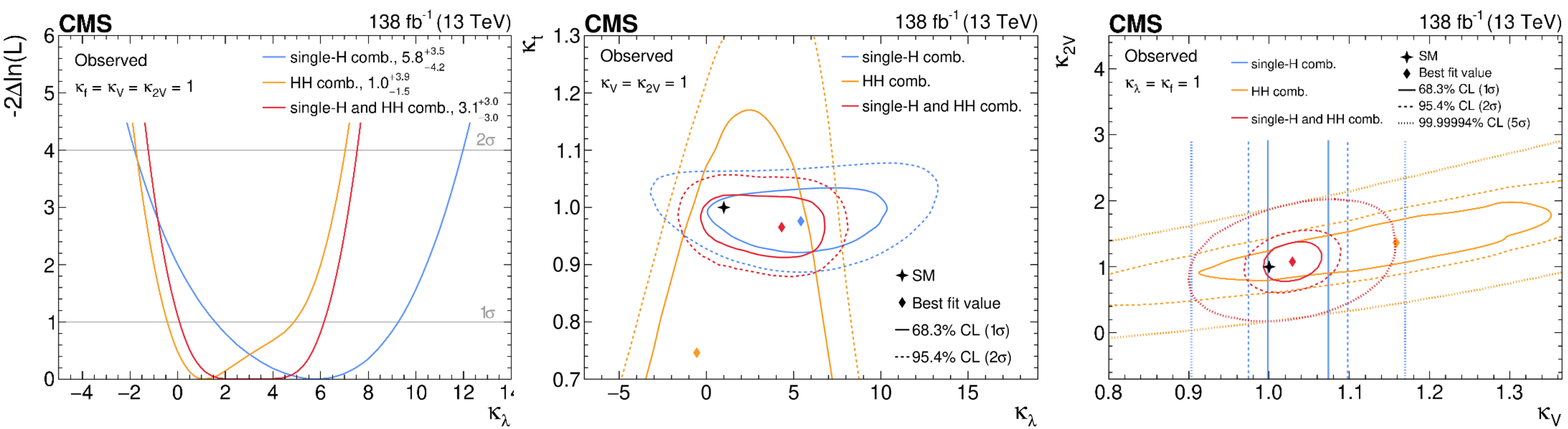

- The combination resolves the degeneracy in k_λ presented in HH-only fits.
- The 2D allowed regions in $(k_\lambda, k_t), (k_V, k_{2V})$ are significantly reduced by H+HH combination

The potential in HL-LHC

Study of Higgs boson pair production is among the most important physics deliverables of HL-LHC

2019 projection of HH in HL-LHC based on early Run2 HH results

LHCXSWG-2019-005

	Statistical-only		**Statistical + Systematic**	
	ATLAS	CMS	ATLAS	CMS
$HH \to b\bar{b}b\bar{b}$	1.4	1.2	0.61	0.95
$HH \to b\bar{b}\tau^+\tau^-$	2.5	1.6	2.1	1.4
$HH \to b\bar{b}\gamma\gamma$	2.1	1.8	2.0	1.8
$HH \to b\bar{b}VV^*$	-	0.59	-	0.56
$HH \to b\bar{b}ZZ(4\ell)$	-	0.37	-	0.37
Combination	3.5	2.8	3.0	2.6
	4.5		4.0	

2025 projection of HH in HL-LHC based on latest Run2 results

HIG-25-002

	2 ab^{-1} ($S2$)		3 ab^{-1} ($S2$)		3 ab^{-1} ($S3$)	
	ATLAS	CMS	ATLAS	CMS	ATLAS	CMS
	HH statistical significance					
$b\bar{b}\tau^+\tau^-$	3.0†	1.9	3.5†	2.4	**3.8†**	**2.7**
$b\bar{b}\gamma\gamma$	2.1†	2.0†	2.4†	2.4†	**2.6†**	**2.6†**
$b\bar{b}b\bar{b}$ resolved	0.9	1.0†	1.0	1.2†	**1.0**	**1.3†**
$b\bar{b}b\bar{b}$ boosted	—	1.8†	—	2.2†	—	**2.2†**
Multilepton	0.8†	—	1.0†	—	**1.0†**	—
$b\bar{b}\ell^+\ell^-$	0.4†	—	0.5†	—	**0.5†**	—
Combination	3.7	3.5	4.3	4.2	**4.5**	**4.5**
ATLAS+CMS	6.0		7.2		**7.6**	

"S2" : uncertainties with statistical origin scaled with luminosity, theory uncertainties halved
"S3": accounting for 5% improvements in b-jets tagging and hadronic taus identification efficiencies

Extensive use of advanced techniques at various stages of analysis in Run2 led to significant gains in sensitivity.

Run 3: a new era of potential for HH

- New triggers designed in Run 3
  - Improves signal efficiency
  - Allows access to more phase spaces for background estimation
- More powerful b-tagging, jet p_T regression and di-jet mass regression methods
  - Heavy-flavour tagging improves ~5% per b-jet at the same mis-tag rate
  - Advanced machine learning methods for jet p_T regression and di-jet mass regression
- Optimization of signal/background classification and categorization
- Improved background estimation, validation, and assessment of systematic uncertainties

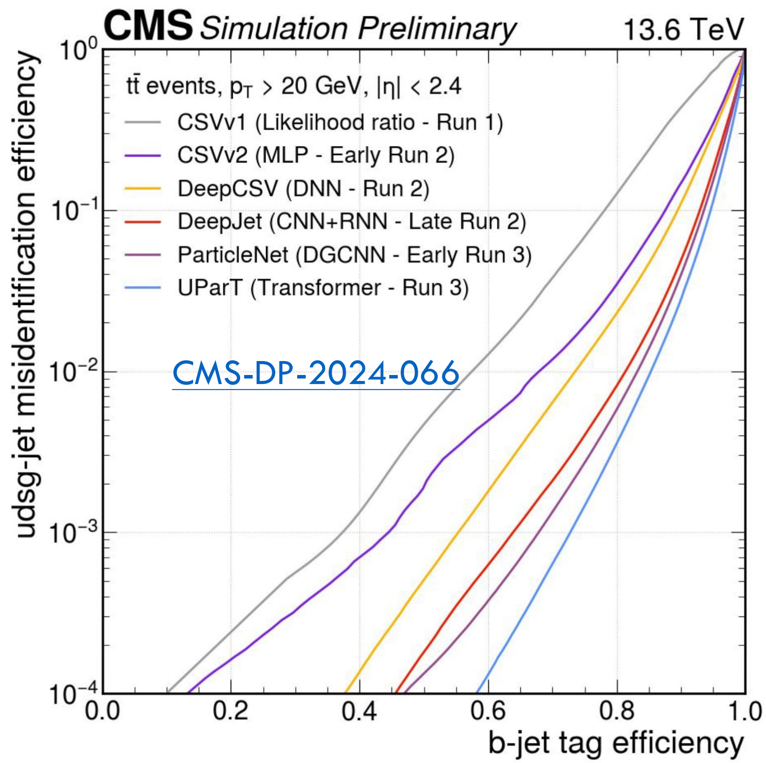

Evolution of the b-tagging performance for identification algorithms used in CMS from Run 1 to Run 3

Huge potential in Run3 HH !

Summary

- Comprehensive HH searches using the full Run 2 dataset at CMS
  - Provide a direct probe of the Higgs potential and rare quartic gauge couplings

- Legacy results show significant sensitivity improvements over early Run 2
  - Expanded exploration of production modes and decay channels, including boosted topologies
  - Extensive application of machine learning for triggers, object tagging and event selection
  - Well-developed EFT interpretation within the HEFT framework
  - Combined analyses with single Higgs processes to constrain k_λ and Higgs couplings simultaneously

- **Looking ahead:** Run 3 holds great potential for further advancing HH searches!

Backup

$HH \rightarrow bbbb$ resolved

- Targeting HH decay resolved into 4 b-jets
- Large multi-jet background estimated from data and fitted simultaneously in multiple signal regions
- Use dedicated BDTs to separate different signals and backgrounds
- Simultaneous fit of MVA for ggF and mHH for VBF categories

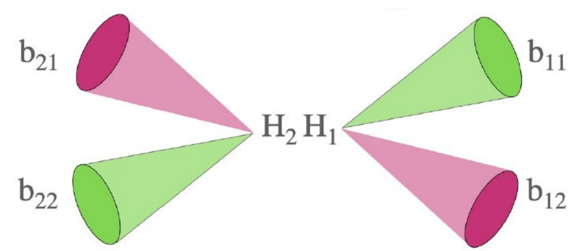

Phys. Rev. Lett. 129 (2022) 081802

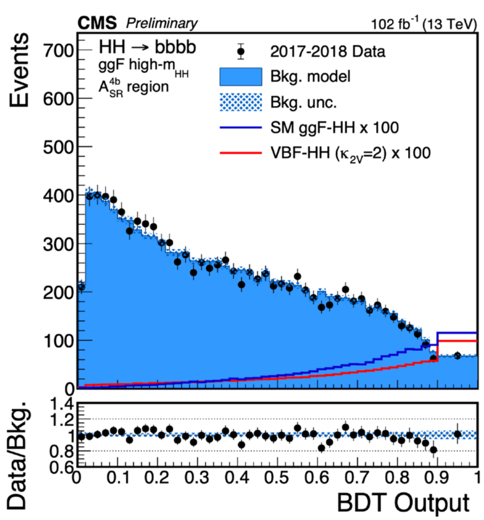

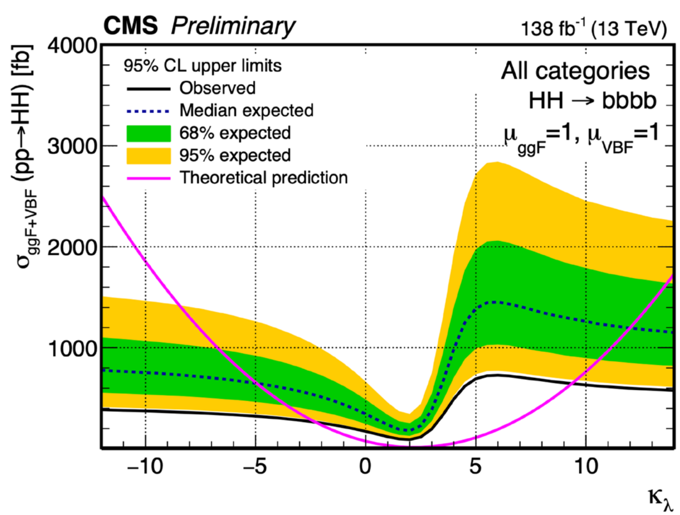

Observed (expected) results:

$$\sigma^{HH}_{ggF+VBF} < 3.9(7.8) \times \sigma^{HH\,SM}_{ggF+VBF}$$

$$-2.3(-5.0) < k_\lambda < 9.4(12)$$

$$-0.1(-0.4) < k_{2V} < 2.2(2.5)$$

$HH \rightarrow bbbb$ boosted

- HH decay boosted into two merged jets
  - Boosted H→bb candidate(s) reconstructed as large radius jet(s)
    - “ParticleNet” tagger (arXiv:1902.08570) to identify boosted H decays
  - DNN b-jet energy regression to improve H→bb mass resolution
- Main backgrounds from QCD and tt
  - Fit/correction from control regions
- ggF and VBF signal extracted with
  - Fit to sub-leading jet mass for ggF
  - Fit to m_{HH} for VBF
- Observed (expected) results:
  - $\sigma_{ggF+VBF}^{HH} < 9.9(5.1) \times \sigma_{ggF+VBF}^{HH\,SM}$
  - $-9.9\ (-5.1) < k_\lambda < 16.9\ (12.2)$
- k_{2V} = 0 firstly excluded at >5σ assuming k_λ = k_t = k_V = 1
  - $0.62\ (0.66) < k_{2V} < 1.41\ (1.37)$

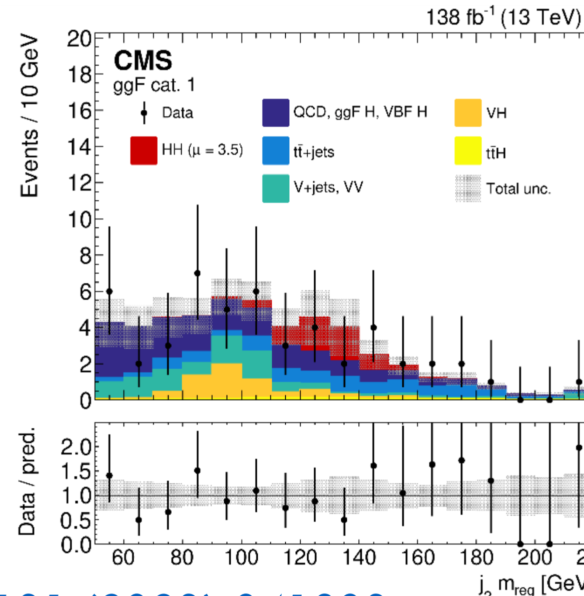

Phys. Rev. Lett. 131 (2023) 041803

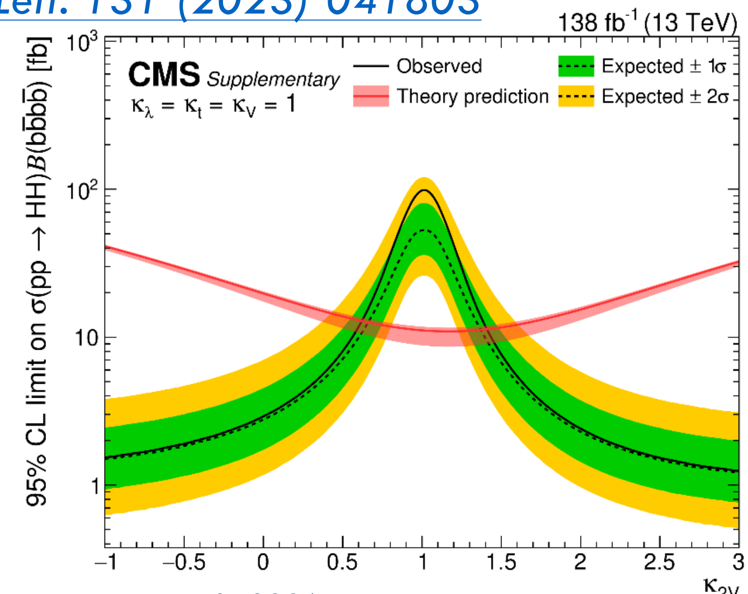

$HH \to bb\tau\tau$

- Targeting HH decays in $\tau_h\tau_h, \mu\tau_h$ and $e\tau_h$
  - Triggers based on leptons and hadronic taus
  - Di-τ trigger with or without jets
  - Single-e, e-τ, single-mu and μ-τ triggers
- Leading background from QCD, ttbar and DY events
  - Estimated using data-driven or control regions
- Event categorization on production mode and final state
- DNN classifiers to separate signal and backgrounds
- Signal extraction from fit to DNN score

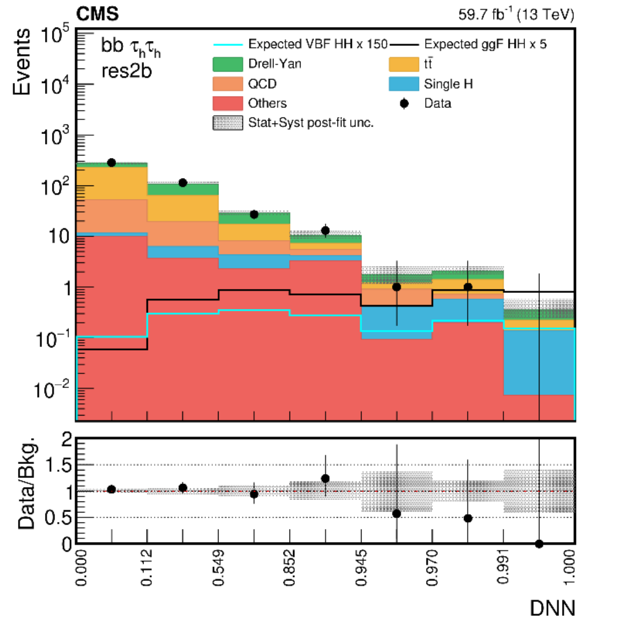

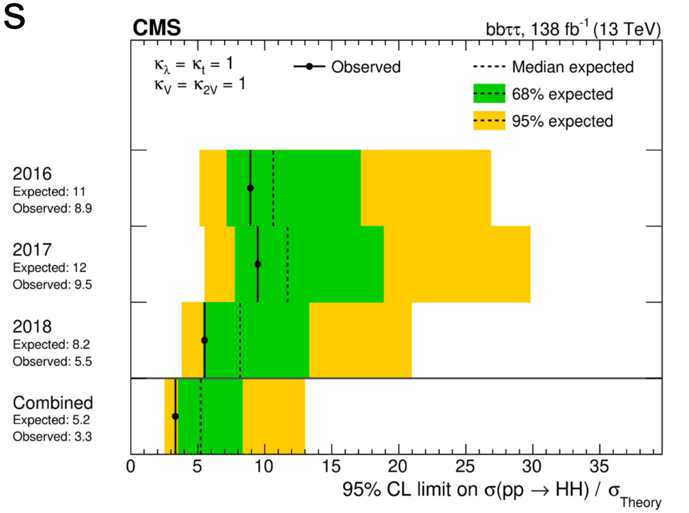

Most stringent limits on inclusive HH (observed) and VBFHH:

$$\sigma^{HH}_{ggF+VBF} < 3.3(5.2) \times \sigma^{HH\,SM}_{ggF+VBF},$$
$$\sigma^{HH}_{VBF} < 124(154) \times \sigma^{HH\,SM}_{VBF},$$

$$-1.8(-3.0) < k_\lambda < 8.8(9.9)$$
$$-0.4(-0.6) < k_{2V} < 2.6(2.8)$$

Phys. Lett. B 842 (2023) 137531

$HH \to bb\gamma\gamma$

- Targeting $HH \to bb\gamma\gamma$ final state analysis
  - very small BR, clean signal extraction due to the narrow $h \to \gamma\gamma$ mass peak
- Main backgrounds: $\gamma\gamma + jets$, $\gamma + jets$, ttH
  - Boosted Decision Trees trained to separate signal and backgrounds
  - Deep Neural Network (DNN) to reduce ttH background
    - ttH: the dominant resonant background, similar final-state topology and can reconstruct a diphoton mass peak resembling the signal
- Category for ggF and VBF based on the MVA output
- Signal extracted from a 2D fit to $(m_{\gamma\gamma}, m_{bb})$

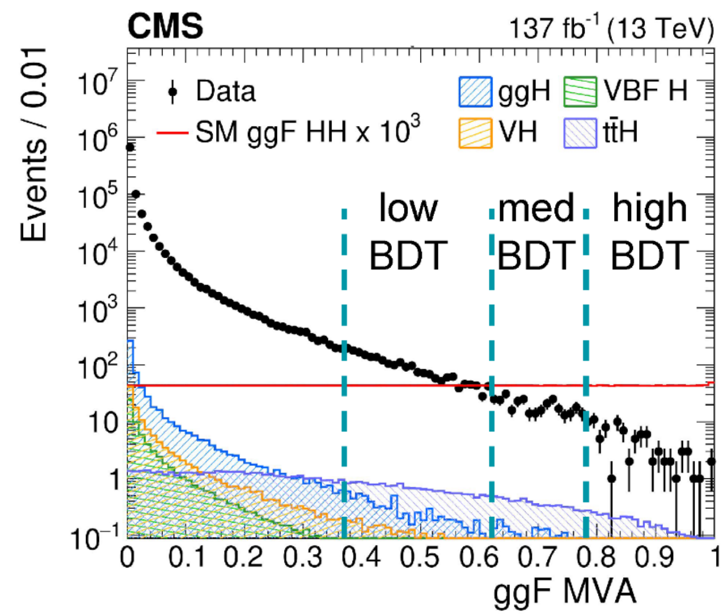

Limit on HH XS×BR vs k_λ

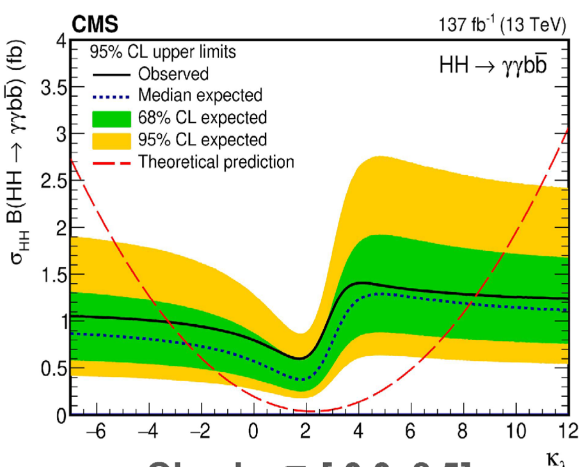

Obs. $k_\lambda \in [-3.3, 8.5]$

Exp. $k_\lambda \in [-2.5, 8.2]$

Limit on VBF HH XS×BR vs $k_{2V} = c_{2V}$, c_{2V}

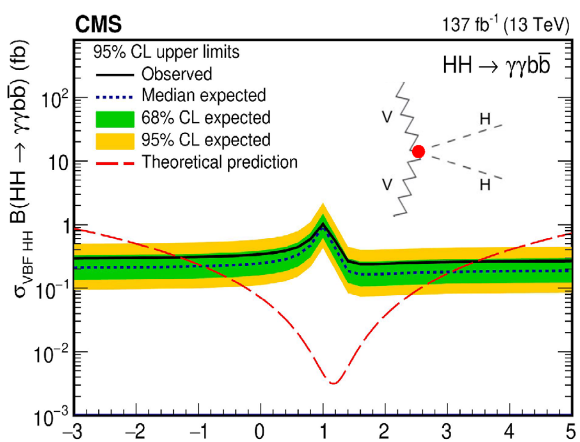

Obs. $k_{2V} \in [-1.3, 3.5]$

Exp. $k_{2V} \in [-0.9, 3.0]$

Obs.(exp.) upper limit on HH signal strength

7.7(5.2)×SM

JHEP 03 (2021) 257

Results from other channels

$VHH\ bbbb$ JHEP 10 (2024) 061

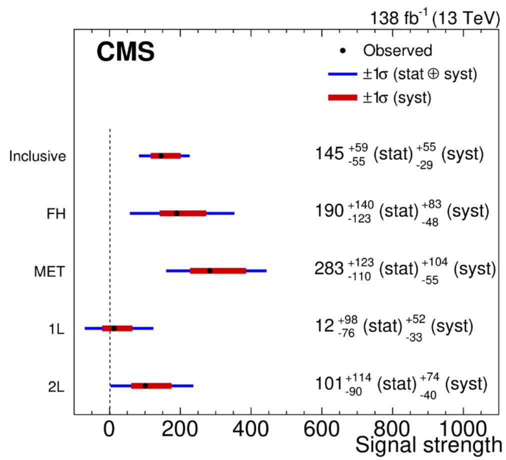

$bbWW(leptonic)$ JHEP 07 (2024) 293

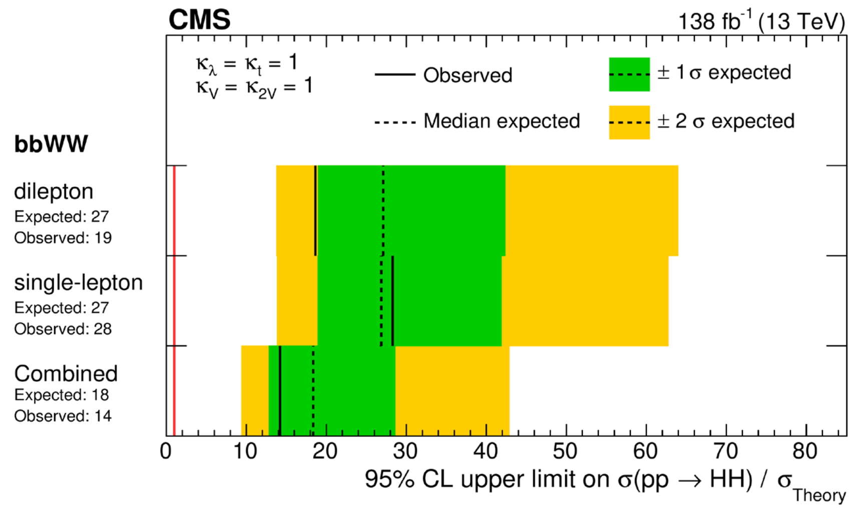

$bbVV(hadronic)$ CMS-PAS-HIG-23-012

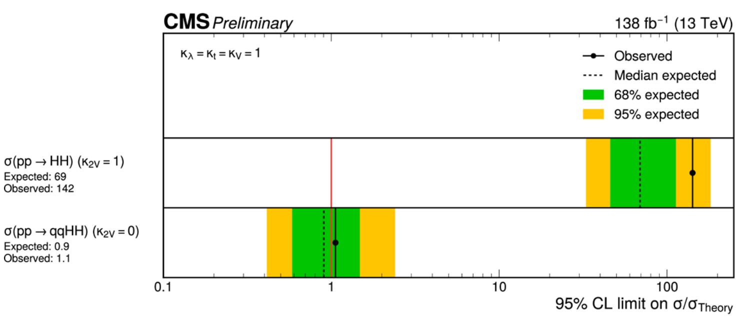

$WW\gamma\gamma$ CMS-PAS-HIG-21-014

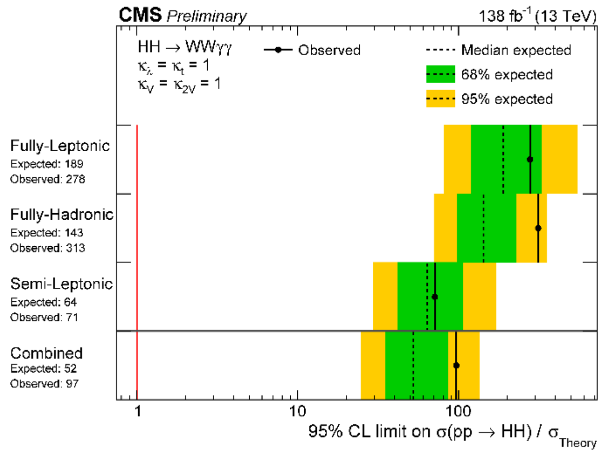

$\tau\tau\gamma\gamma$ CMS-PAS-HIG-22-012

Observed (expected) HH upper limit at the 95% CL: $33(26) \times \sigma_{ggF+VBF}^{HH\ SM}$

Complementary HH searches, with results compatible with SM predictions

H+HH combination

- H+HH combination
  - Ultimate precision on k_λ with less assumptions
  - Simultaneously constraining k_λ and modifiers of SM H couplings to fermions, and vector bosons
  - The main channels of single Higgs and HH are included

Analysis	Integrated luminosity (fb^{-1})	Targeted H production modes	Maximum granularity	References
$\mathrm{H} \to 4l$	138	ggF, VBF, VH, $\mathrm{t\bar{t}H}$	STXS 1.2	[51]
$\mathrm{H} \to \gamma\gamma$	138	ggF, VBF, VH, $\mathrm{t\bar{t}H}$, tH	STXS 1.2	[52,none]
$\mathrm{H} \to \mathrm{WW}$	138	ggF, VBF, VH	STXS 1.2	[54]
$\mathrm{H} \to$ leptons ($\mathrm{t\bar{t}H}$)	138	$\mathrm{t\bar{t}H}$	Inclusive	[55]
$\mathrm{H} \to \mathrm{b\bar{b}}$ (ggF)	138	ggF	Inclusive	[56]
$\mathrm{H} \to \mathrm{b\bar{b}}$ (VH)	77	VH	Inclusive	[48]
$\mathrm{H} \to \mathrm{b\bar{b}}$ ($\mathrm{t\bar{t}H}$)	36	$\mathrm{t\bar{t}H}$	Inclusive	[57]
$\mathrm{H} \to \tau\tau$	138	ggF, VBF, VH	STXS 1.2	[58]
$\mathrm{H} \to \mu\mu$	138	ggF, VBF	Inclusive	[59]

Analysis	Int. luminosity (fb^{-1})	Targeted HH production modes	References
$\mathrm{HH} \to \gamma\gamma\mathrm{b\bar{b}}$	138	ggF and VBF	[53]
$\mathrm{HH} \to \tau\tau\mathrm{b\bar{b}}$	138	ggF and VBF	[60]
$\mathrm{HH} \to \mathrm{b\bar{b}b\bar{b}}$	138	ggF, VBF, and VHH	[61,62,none]
$\mathrm{HH} \to$ leptons	138	ggF	[64]
$\mathrm{HH} \to \mathrm{WWb\bar{b}}$	138	ggF and VBF	[65]

Run 3 $HH \rightarrow 4b$ resolved analysis

- Targeting HH decay resolved into 4 AK4 b-jets   CMS-PAS-HIG-24-010
- Backgrounds: >90% QCD multijets, <10% ttbar, <1% for others like H, V+jets and diboson processes

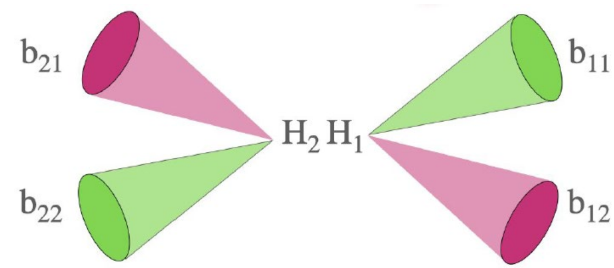

- Analysis strategy
  - Event pre-selection
    - Dedicated triggers, 4 jet selection and HH candidate reconstruction with jet paring and regression
  - Selection of signal regions (SRs) and control regiosn (CRs) based on m_{H1}, m_{H2}, and b-multiplicity
  - Fully data-driven background prediction in SR
    - Mapping from lower N_{bjet} CRs to SRs using MVAs trained in other CRs
  - Multi-classifier MVAs to classify different events and discriminant signal/backgrounds
  - Signal extracted via likelihood fit to the data using the MVA score
    - Targeting both ggF categories, and VBF categories with ggF suppression
- Two different approaches explored
  - Different definition of SRs and CRs as the second targets also ZH and ZZ processes
  - Different ML algorithms used in background estimation, event classification and background rejection

Run 3 $HH \to 4b$ resolved analysis – approach 1

[CMS-PAS-HIG-24-010]

- SRs and CRs defination
  - Number of b jets, position in m_{H1}-m_{H2} mass plane
- Data-driven background estimation
  - DNN trained to map backgrounds from CR_{2b} to CR_{4b}, then applied to SR_{2b} to prediction backgrounds in SR_{4b}
  - Background model from ensemble 20 individual background predictions
    - Helps to reduce and quantify variance in bkg. prediction
- Background uncertainty and validation
  - Fit differences among statistically independent predictions
  - Validated in both 3b CRs and 4b validation regions
- Customized ParticleTransformer to separate HH→4b signal from background
  - With transformer blocks using jet-based input features
  - Trained using simulated signal for mix of λ hypotheses
- Signal extracted via binned maximum-likelihood fit of classifier score distribution in SR_{4b}
  - Binning chosen with uniformed signal contribution

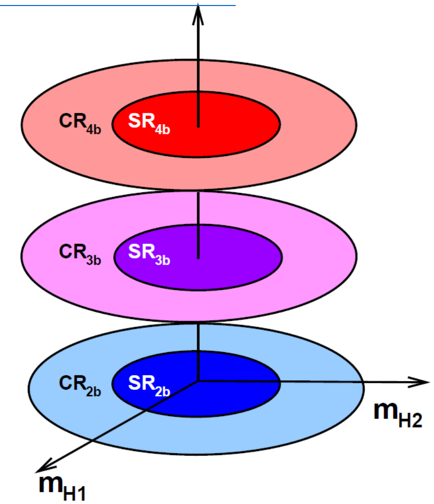

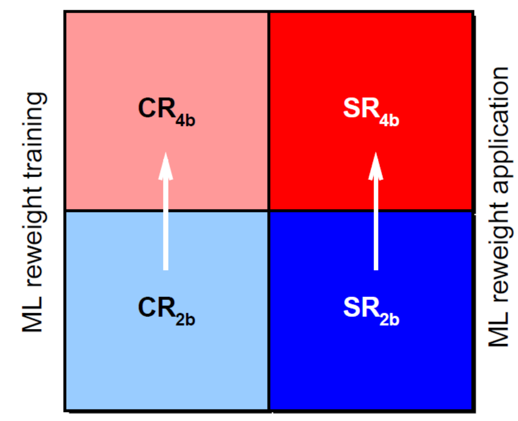

Run 3 $HH \to 4b$ resolved analysis – approach 2

- Targets HH and also ZH and ZZ processes
  - SRs & CRs definition
    - Number of Loose (L), Medium (M), and Tight (T) b jets
    - m_{H1} & m_{H2}
- FeynNet, graph-based neural network, used for:
  - Background estimation and validation
  - Classify HH (ggHH+qqHH), ZH, & ZZ processes
  - Signal-vs-background (SvB) discrimination
- Background estimation
  - SR_{3T1M} region: reweight SR_{2b} with mapping learned by FeynNet from CR_{2b} to CR_{3T1M}
  - SR_{3T1L} region: reweight SR_{3MnT} with mapping learned by FeynNet from CR_{3MnT} to CR_{3T1L}
- Background uncertainty estimation and validation
  - Fit differences with 30 trained bkg. models
  - Fit the average of bkg models to the observed data in SR_{3MnT}
  - Validated with ZZ, ZH→4b processes
- Signal extracted from the fit with SvB discriminant score

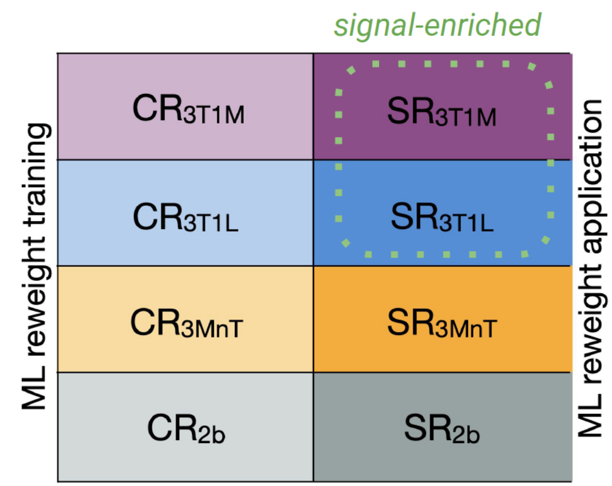

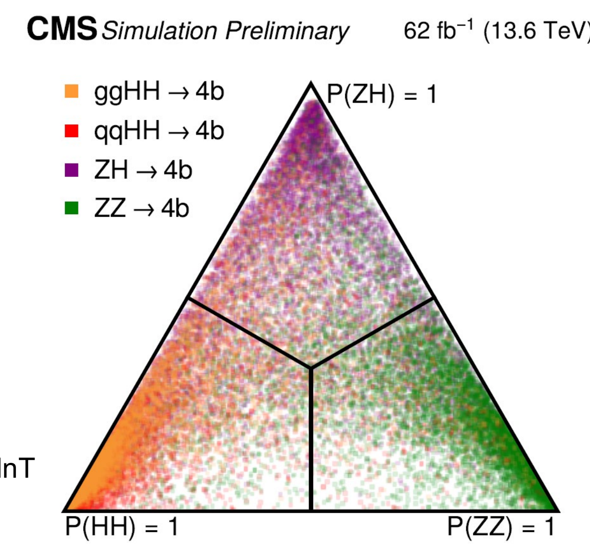

$HH \to 4b$ resolved results with 62 fb^{-1} data (2022+2023)

- Expected best fit of signal strength and upper limits @ 95% C.L.

	μ_{HH}		μ_{ggHH}		μ_{qqHH}	
Expected	Best-fit	U.L.	Best-fit	U.L.	Best-fit	U.L.
First approach	$1.0^{+2.6}_{-2.4}$	5.3	$1.0^{+2.6}_{-2.4}$	5.3	1^{+46}_{-39}	94
Second approach	$1.0^{+2.9}_{-2.7}$	6.1	$1.0^{+3.0}_{-2.7}$	6.2	1^{+58}_{-50}	128

- Observed best fit of signal strength and upper limits @ 95% C.L.

	μ_{HH}		μ_{ggHH}		μ_{qqHH}	
Observed	Best-fit	U.L.	Best-fit	U.L.	Best-fit	U.L.
First approach	$0.9^{+2.6}_{-2.4}$	6.3	$0.9^{+2.6}_{-2.4}$	6.4	-3.0^{+45}_{-39}	93
Second approach	$-1.3^{+2.7}_{-2.9}$	5.0	$-1.1^{+2.7}_{-2.9}$	5.2	-62^{+46}_{-44}	81

- Observed and expected 95% CL intervals for κ_λ and κ_{2V}

95% CL interval	κ_λ		κ_{2V}	
	Obs.	Exp.	Obs.	Exp.
First approach	$[-4.4, 11.7]$	$[-3.8, 11.0]$	$[-0.08, 2.20]$	$[-0.08, 2.19]$
Second approach	$[-3.2, 10.0]$	$[-4.4, 11.6]$	$[-0.05, 2.24]$	$[-0.25, 2.4]$

CMS-PAS-HIG-24-010

- Results are compatible between two approaches
- More than a factor of 2 improvements comparing to Run2 results scaled to the same luminosity

Run 3 $HH \rightarrow 4b$ boosted analysis

- Targeting HH decay boosted into two merged jets
  - With both ggF and VBF topologies
- Analysis strategy
  - Event preselection with AK8 jets using GloParT scores
  - Split into SRs & CRs with two different strategies
  - 1. Based on H→bb candidate masses & sub-leading bb-tag score, and signal extracted with **two complementary fit methods**
    - Mass-fit analysis: categorize events by SvsB DNN score and H2 bb-tag, then fit $m(H_2)$
    - DNN-fit analysis: categorize events by H_2 bb-tag only, then fit SvsB DNN score distribution
    - **Novel background model, re-designed data-driven analysis strategy, exclusive VBF channels**
  - 2. Based on BDT multi-classifier & GloParT score, and signal extracted via mass fit on Jet 2
    - **Similar to Run2 with new triggers & GloParT for bb-tagging**

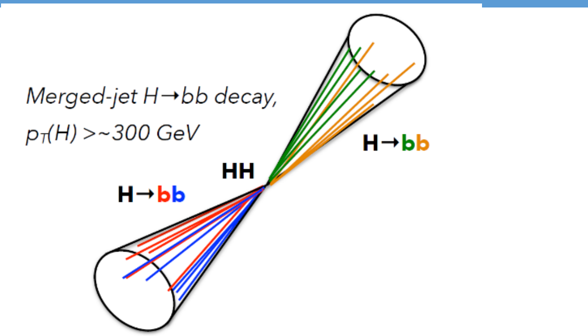

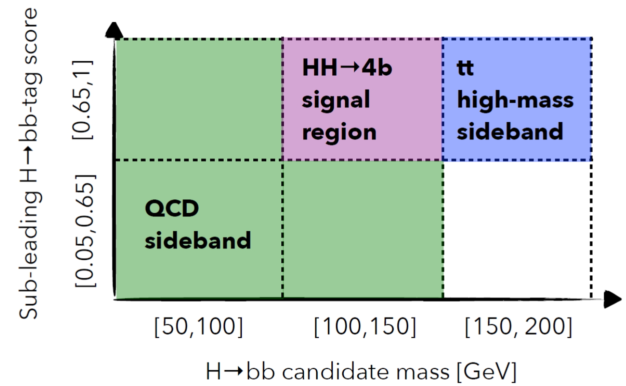

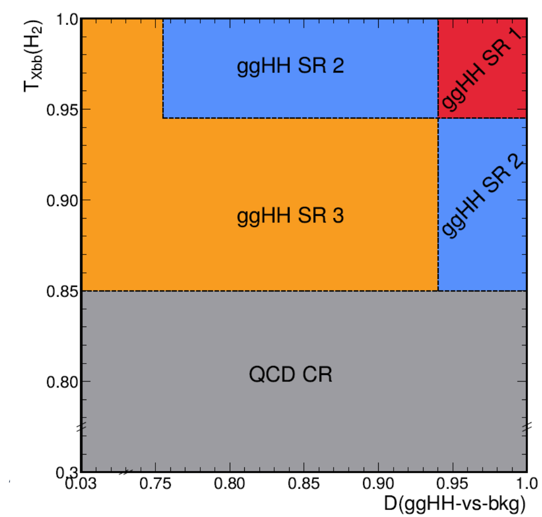

[CMS-PAS-HIG-24-010]

$HH \to 4b$ boosted results with 62 fb^{-1} data (2022+2023)

- The expected best-fit signal strengths and 95% CL upper limits

	μ_{HH}		μ_{ggHH}		μ_{qqHH}	
Expected	Best-fit	U.L.	Best-fit	U.L.	Best-fit	U.L.
First approach (mass-fit)	$1.0^{+3.4}_{-2.9}$	7.1	$1.0^{+3.5}_{-3.0}$	7.3	1^{+83}_{-67}	173
First approach (DNN-fit)	$1.0^{+3.1}_{-2.6}$	6.6	$1.0^{+3.2}_{-2.7}$	6.7	1^{+82}_{-66}	185
Second approach	$1.0^{+3.7}_{-3.1}$	8.1	$1.0^{+3.8}_{-3.2}$	8.3	1^{+224}_{-194}	518

- The observed best-fit signal strengths and 95% CL upper limits

	μ_{HH}		μ_{ggHH}		μ_{qqHH}	
Observed	Best-fit	U.L.	Best-fit	U.L.	Best-fit	U.L.
First approach (mass-fit)	$-2.6^{+2.9}_{-3.2}$	5.3	$-2.5^{+2.9}_{-3.2}$	5.5	-56^{+45}_{-65}	131
First approach (DNN-fit)	$-0.8^{+2.7}_{-2.5}$	5.8	$-0.8^{+2.7}_{-2.6}$	6.1	-68^{+45}_{-65}	131
Second approach	$2.1^{+4.5}_{-3.7}$	11.1	$2.0^{+4.6}_{-3.8}$	11.2	408^{+188}_{-230}	1060

- Observed and expected 95% CL intervals for κ_λ and κ_{2V}

95% CL interval	κ_λ		κ_{2V}	
	Obs.	Exp.	Obs.	Exp.
First approach (mass-fit)	$[-5.1, 10.9]$	$[-6.8, 12.8]$	$[0.63, 1.42]$	$[0.54, 1.51]$
First approach (DNN-fit)	$[-6.5, 13.4]$	$[-7.7, 14.9]$	$[0.64, 1.41]$	$[0.56, 1.49]$
Second approach	$[-11.0, 19.2]$	$[-10.3, 18.4]$	$[0.30, 1.74]$	$[0.47, 1.58]$

CMS-PAS-HIG-24-010

- Constraints on K2V comparable to those from the larger Run 2 data set

$HH \rightarrow 4b$ combined results with 62 fb^{-1} data (2022+2023)

- Combination of resolved and merged topologies
  - Using approach 1 with the best expected sensitivity

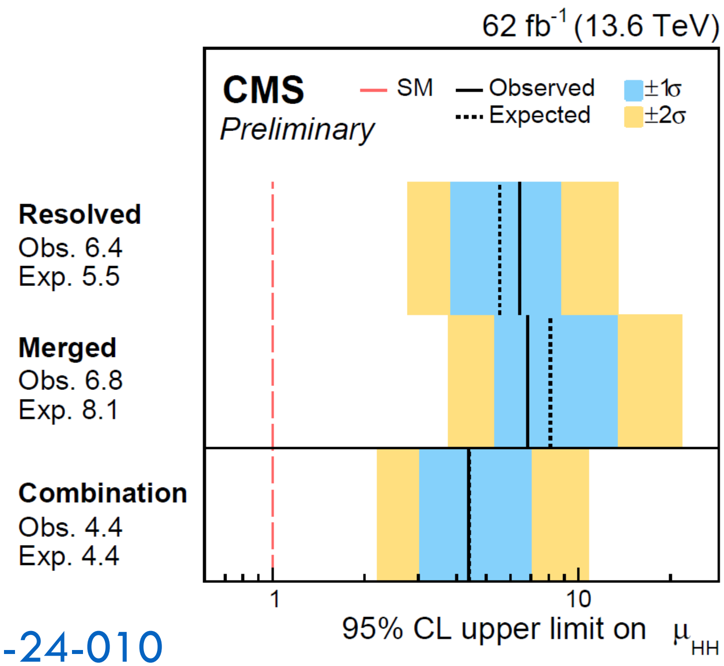

- Observed (expected) 95% CL Upper limits on the HH signal strength μ_{HH}: $4.38\ (4.39)$
- Observed (expected) k_λ range at 95% CL: $-3.3\ (-3.4) < k_\lambda < 10.0\ (7.89)$
- Observed (expected) k_{2V} range at 95% CL: $0.63\ (0.54) < k_{2V} < 1.43\ (1.51)$

CMS-PAS-HIG-24-010

- Results are consistent with the SM prediction
- Significant improvements on the analysis sensitivity thanks to novel analysis techniques implemented

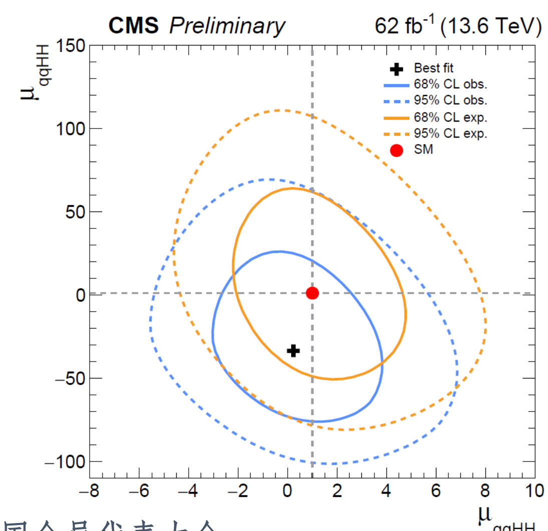

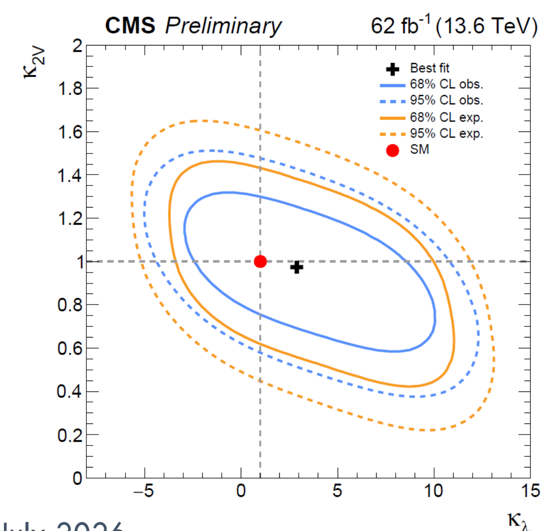

Run3 $HH \to bb\gamma\gamma$ analysis

- Targeting $bb\gamma\gamma$ final state analysis
- **Overview of the analysis strategy**

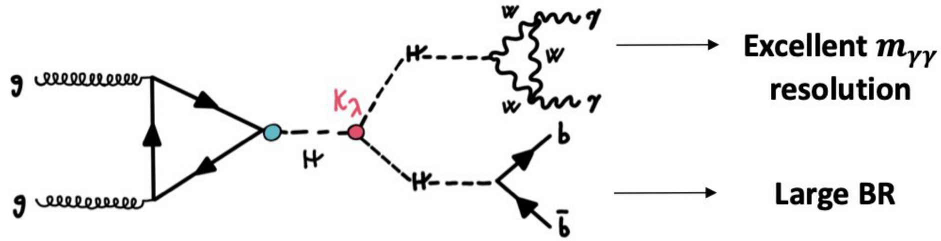

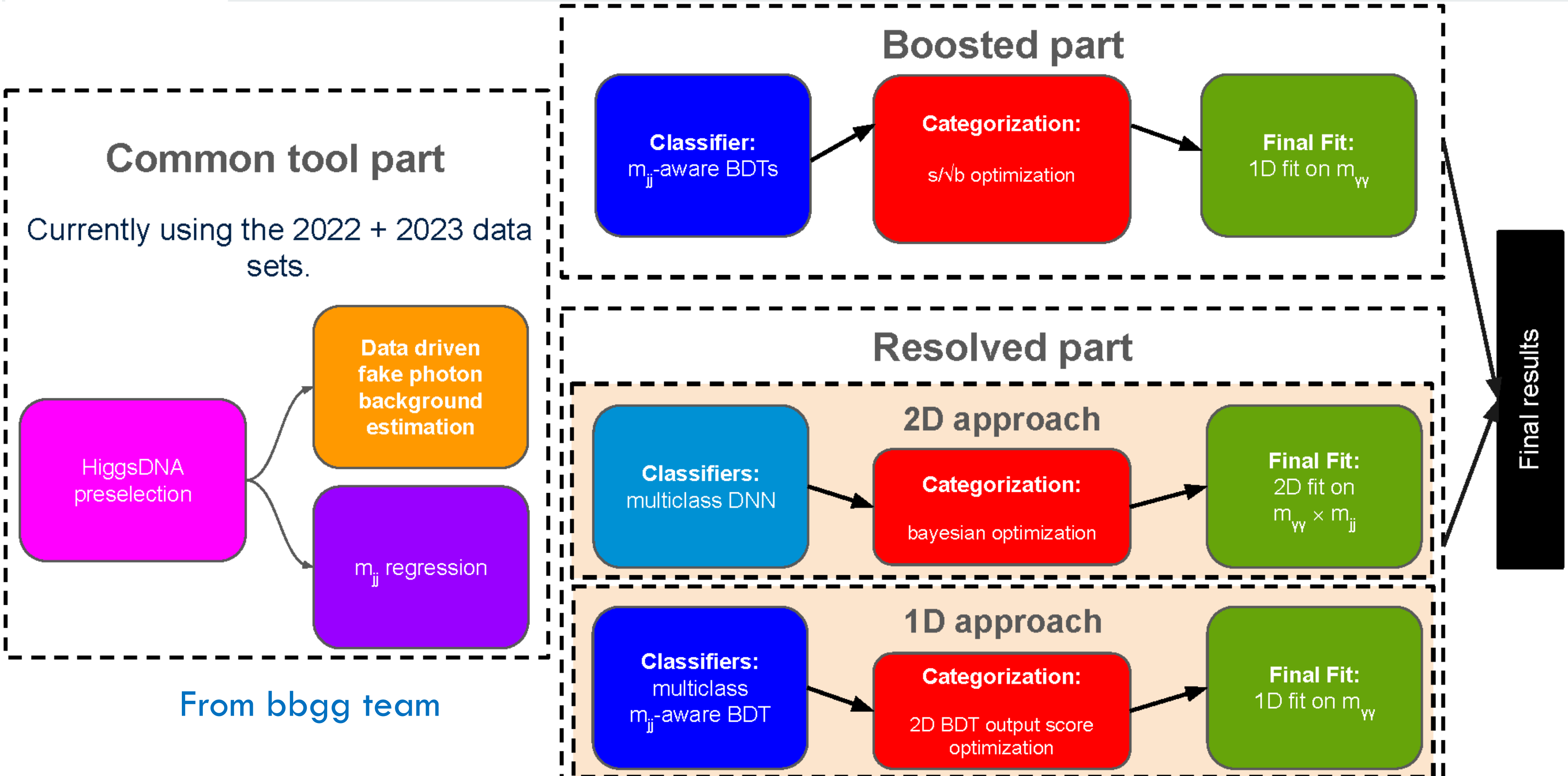

Run3 $HH \rightarrow bb\gamma\gamma$ analysis

- Pre-selections
  - Photon pre-selection targeting H→γγ signatures
    - Kinematic selections + H→γγ candidate chosen as the highest sum p_T pair
  - Loose jet pre-selection targeting H→bb signatures
    - Kinematic selections + H→bb candidate chosen as the highest PNet b-tagging score pair
- Dijet mass regression
  - Dedicated DNN regressor developed for dijet mass regression
  - Improved the dijet mass resolution ~20% (w.r.t PNet reg.)
- Data-driven method for fake-photon backgrounds
  - Improve background models used in MVA training and analysis optimization
  - Extract a PDF function from low γ MVA ID sidebands to re-weight data events with non prompt γ in the preselection region
  - Template fitting of non-resonant bkg to Data in sidebands to further improve yield agreement

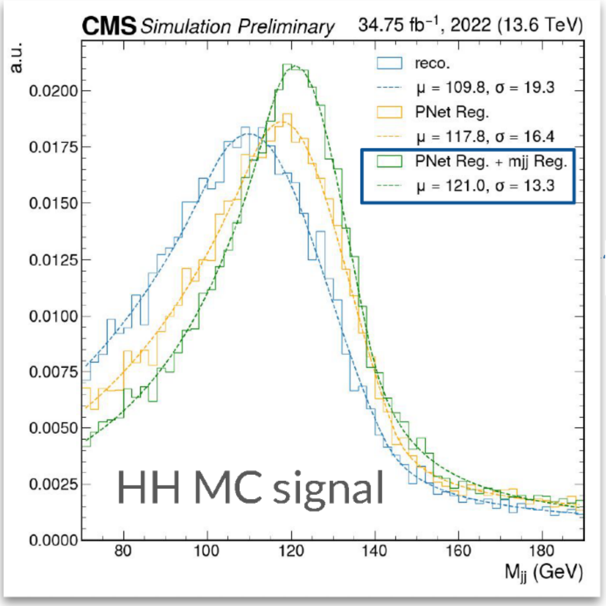

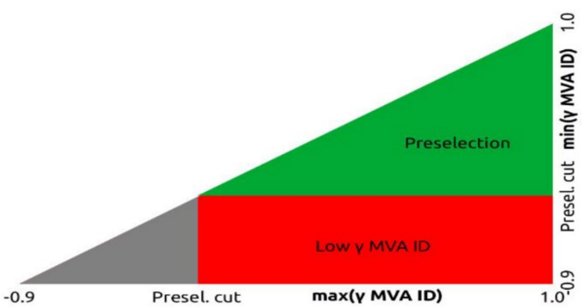

Run3 $HH \to bb\gamma\gamma$ analysis – resolved 1D

- A multiclass BDT with mjj as input trained to separate signal and backgrounds
  - Backgrounds categorized into 3 classes:
    - Non-resonant QCD & γ(γ)+jets & ggH & VBF H, ttH & bbH, VH

CMS-PAS-HIG-25-007

- Optimize 3 categories based on discriminators, D_{QCD} and D_{ttH}, to maximize S/B
  - $D_{QCD} = \frac{P_{HH}}{P_{HH}+P_{QCD}+P_{VH}}$, $D_{ttH} = \frac{P_{HH}}{P_{HH}+P_{ttH}}$, where P is the multiclass BDT score
- Signal extracted by performing a fit to the diphoton mass distribution $m_{\gamma\gamma}$
  - Signal and resonant backgrounds: modeled using the sum of N Gaussian functions
  - Nonresonant background: modeled with a set of smooth exponentially falling functions
    - Discrete profiling employed to determine best-ft backgrounds and their systematic uncertainties

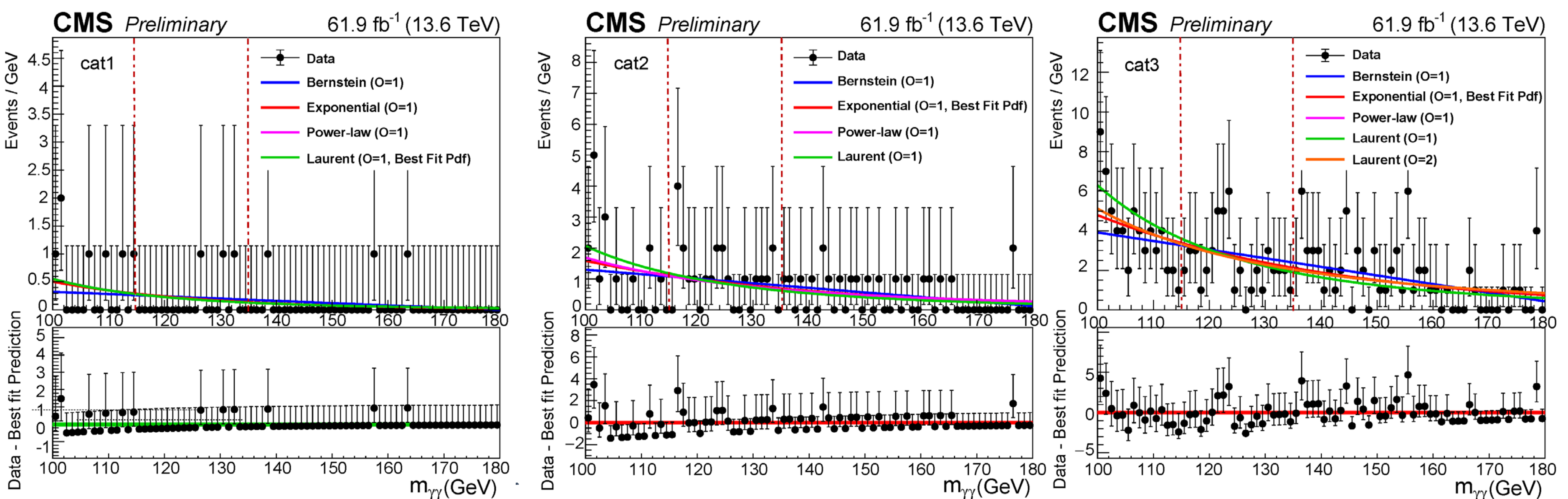

Run3 $HH \to bb\gamma\gamma$ analysis – resolved 2D

- A multiclass DNN trained wo. $m_{\gamma\gamma}$ or m_{jj} as inputs
  - Backgrounds categorized into 3 classes:
    - Nonresonant bkgs (QCD + γ+jets, γγ+tt/jets), ttH, Other single H bkgs
- Bayesian optimization of categories based on DNN outputs
  - Maximise the asymptotic significance (Z) with MC + data-driven backgrounds
  - Cumulative significance plateaus after 3 SRs
- Signal extracted by a 2D fit of $m_{\gamma\gamma}$ and m_{jj}
  - Non-resonant background: smoothly falling functions + discrete profiling method
  - Signal: a sum of Gaussians
  - Resonant background: Double Crystal Ball for VH and ttH
  - 2D fit built as the product of the two 1-D distributions
    - Extra uncertainties to include bias introduced by neglecting correlations

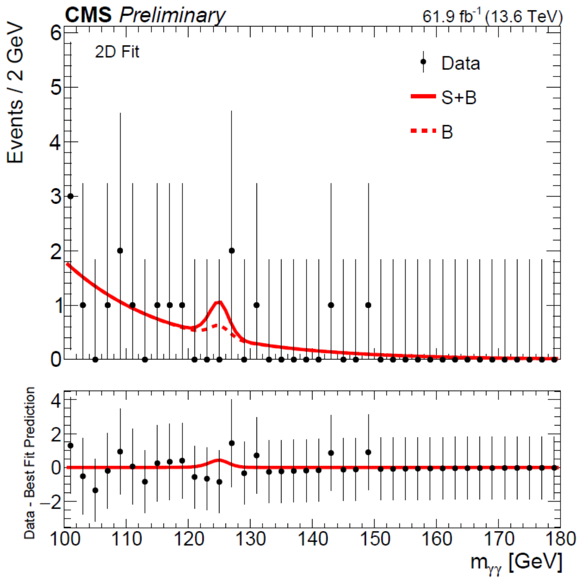

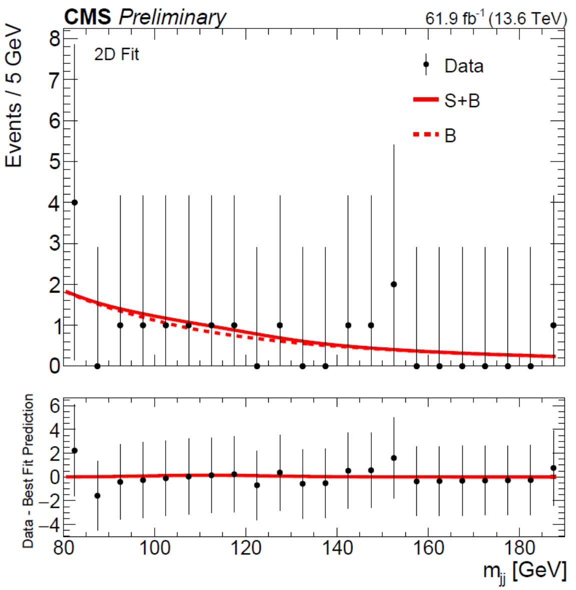

CMS-PAS-HIG-25-007

Run3 $HH \to bb\gamma\gamma$ analysis – boosted

- Novel boosted topologies also explored in Run3 $HH \to bb\gamma\gamma$ analysis
  - Exploit HH production with a high-pT $H \to bb$ candidate in the final state
  - Defined by requiring the presence of at least one selected AK8 jet
- A BDT trained to discriminate signal against background
- 1 boosted category optimized by maximizing expected upper limit using the BDT score
  - Prioritize events falling in the "boosted" category by removing overlapped events from the other non-boosted categories
- Signal extracted by 1D fit due to limited statistics
  - Non-resonant background: smoothly falling functions + discrete profiling method
  - Resonant bkgs and signal: Double Crystal Ball (DCB) functional forms

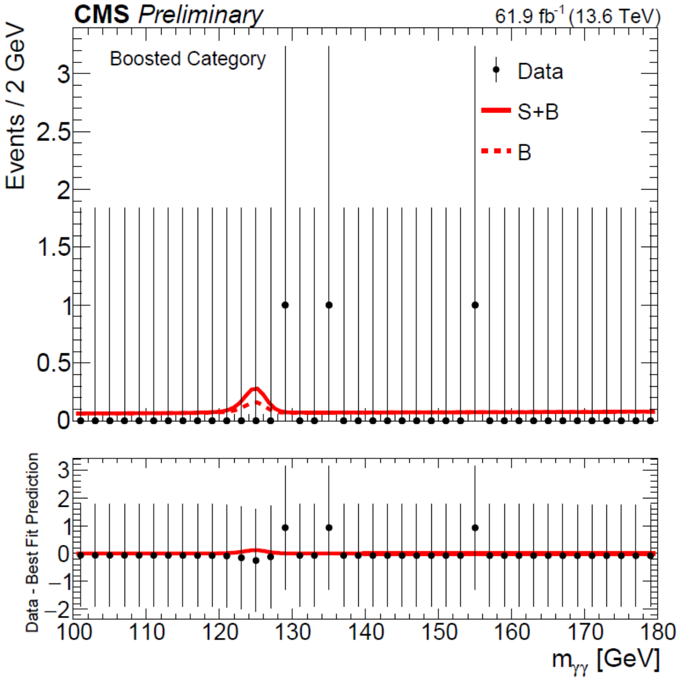

CMS-PAS-HIG-25-007

$HH \to bb\gamma\gamma$ analysis results with 62 fb^{-1} data (2022+2023)

- The combination of the boosted and resolved **1D** strategy categories
  - Observed (expected) 95% CL upper limit: 7.4 (8.7) times the SM cross section.
  - Observed (expected) 95% CL bounds on k_λ : [-3.9, 10.4] ([-4.5, 11.1])
  - ~ 5% better adding the boosted category

CMS-PAS-HIG-25-007

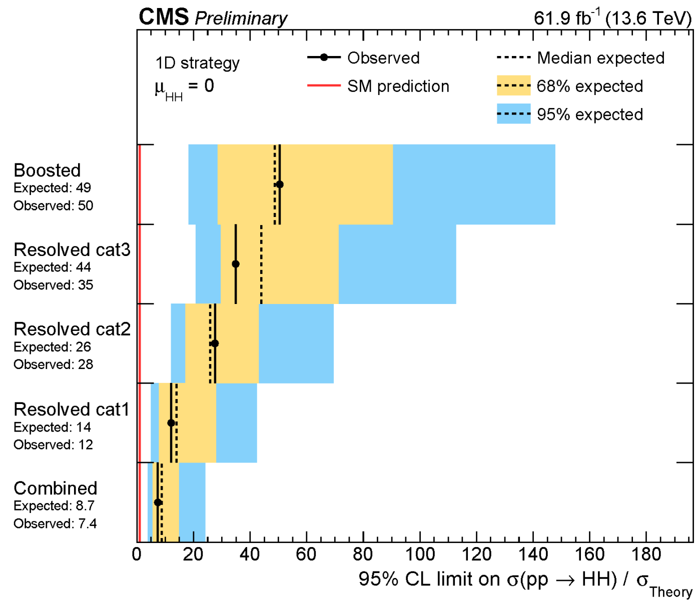

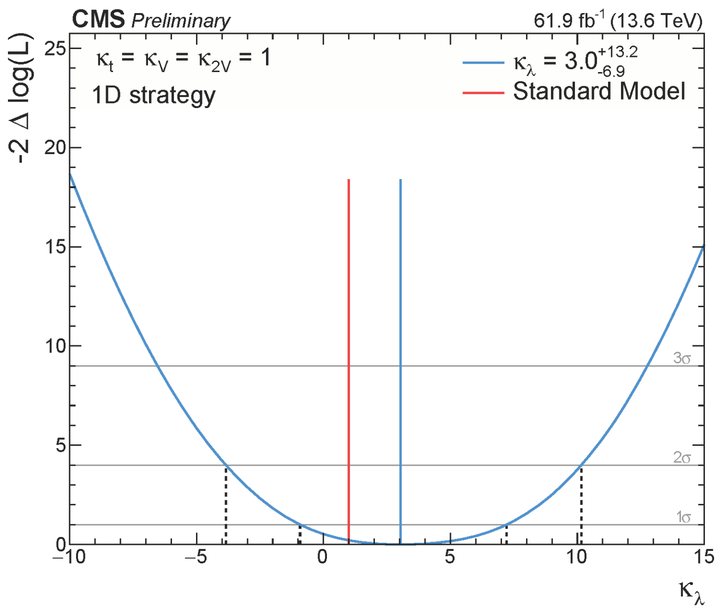

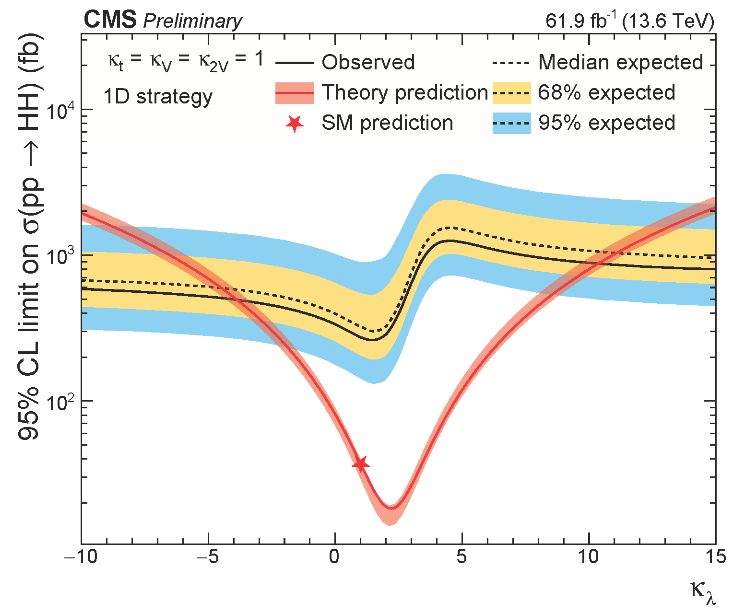

$HH \rightarrow bb\gamma\gamma$ analysis results with 62 fb^{-1} data (2022+2023)

- The combination of the boosted and resolved **2D** strategy categories
  - Observed (expected) 95% CL upper limit: 11.0 (7.3) times the SM cross section.
  - Observed (expected) 95% CL bounds on k_λ : [-5, 12] ([-3.6, 10.5])
- Leading uncertainties are background statistic uncertainties and HH theoretical uncertainties

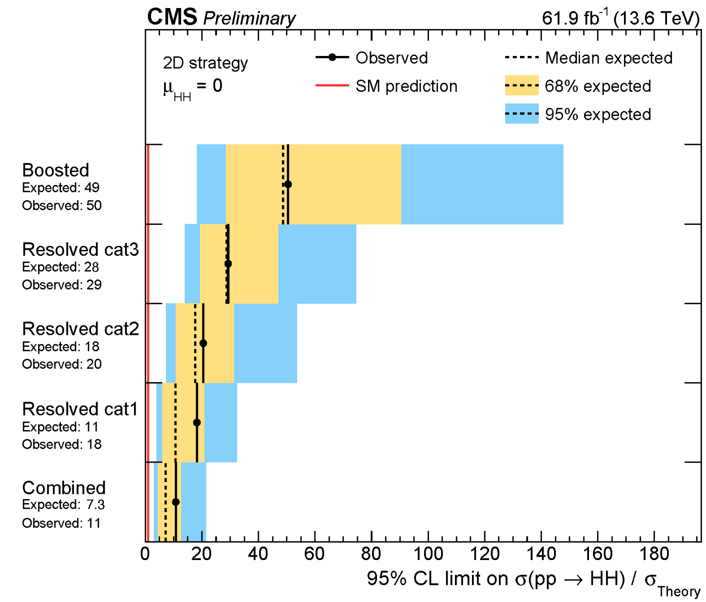

CMS-PAS-HIG-25-007

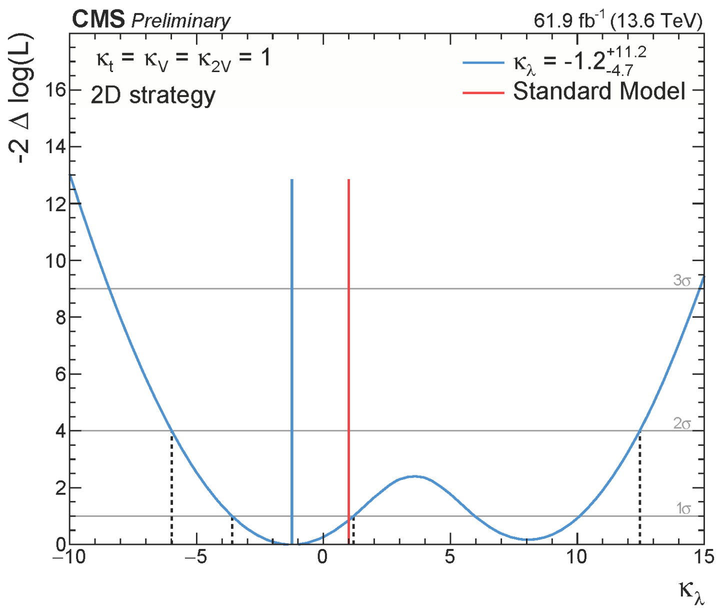

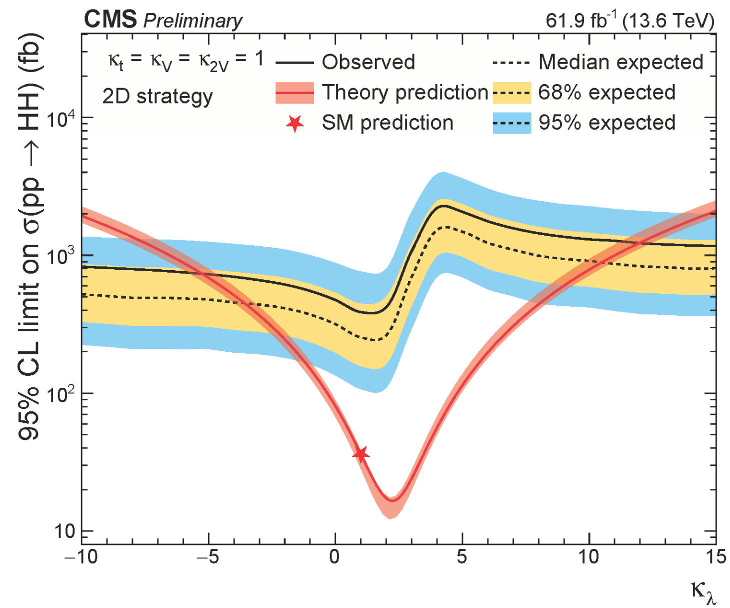

Overview of the improvements in Run 3 HH analysis

- **New triggers**: **e.g.** > factor 2 absolute HH→4b trigger efficiency for Run3, expanded analysis phase space
- **b-tagging and jet p_T regression**: PNET improves heavy-flavour tagging (±5% per b-jet at same mis-tag) and introduces a ML flavour dependent jet p_T regression
- **Improved jet paring and di-jet mass resolution**
- New development in signal/background classification and categorization, background modeling, validation and uncertainty estimation
- Novel boosted topologies in some channels

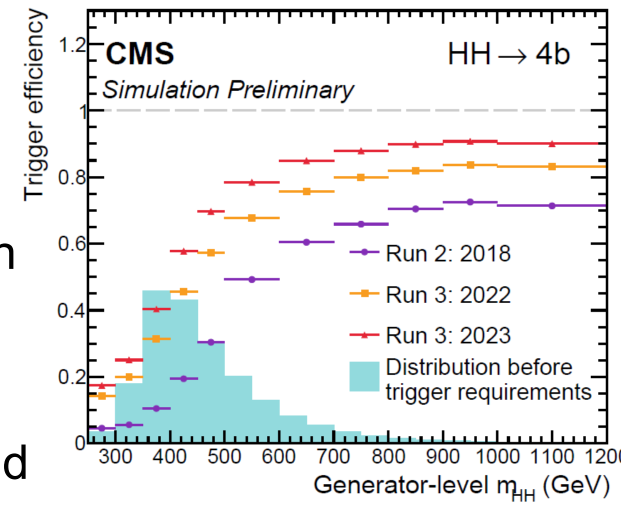

CMS-PAS-HIG-24-010

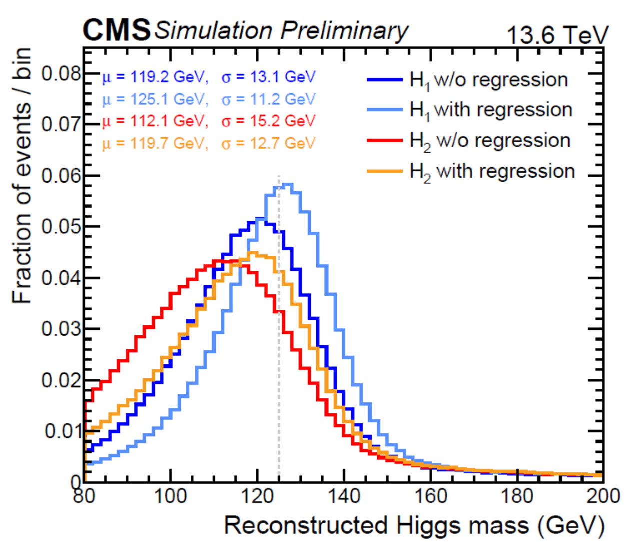

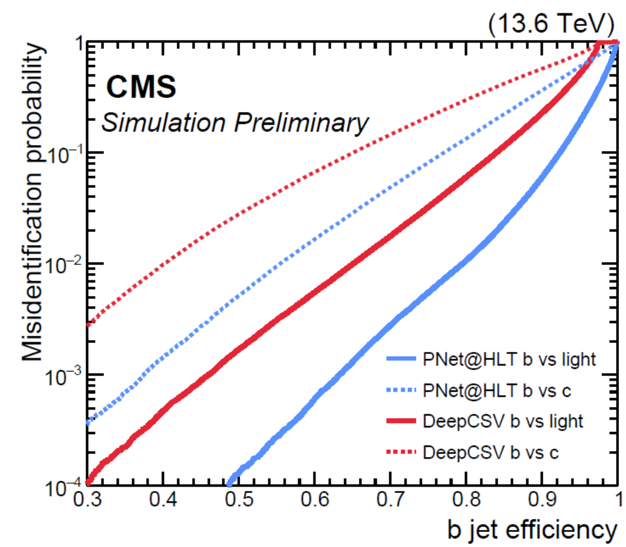

HH Combination of ATLAS and CMS at 13 TeV

- HH combination between CMS and ATLAS at 13TeV: arXiv:2602.23991
  - Using full Run 2 data ranging between 126 and 140 fb^{-1}
  - With the main channels in both analyses
  - Observed (expected under the background-only hypothesis) 95% CL Upper limits on $\sigma_{HH}/\sigma_{Theory}$: $2.5\ (1.7)$
  - Signal strength: $0.8^{+0.9}_{-0.7}$
  - Observed (expected with SM HH) k_λ range at 95% CL: $-0.71\ (-1.3) < k_\lambda < 6.1\ (6.7)$
  - Observed (expected with SM HH) k_{2V} range at 95% CL: $0.73 (0.66) < k_{2V} < 1.3\ (1.40)$
  - Compatible results between CMS and ATLAS
  - The most sensitive HH production results to date
    - The expected limits are approaching unity with a mild excess of about 1σ observed under the background-only hypothesis.